A developed model updating method based on extended frequency response functions and its application study of offshore structures

Fushun Liu[a,b,*], Xingguo Li[a], Hong Song[a], Dianzi Liu[c]

[a]College of Engineering, Ocean University of China, Qingdao 266100 , China
[b]Shandong Province Key Laboratory of Ocean Engineering, Ocean University of China, Qingdao 266100, China
[c]School of Engineering, University of East Anglia, Norwich, NR14 7TH, United Kingdom

---

Abstract

Accurate finite element (FE) models are extremely vital to the analysis of the dynamic characteristics of engineering structures. However, it is challenging for the frequency response function(FRF)-based model updating method to obtain reliable numerical results as the limited number of FRFs at the selected peak positions usually leads to an unacceptable or failure of model updating. Moreover, the increased number of updating coefficients in complex engineering problems generates nonlinear optimization models with the local solutions by traditional optimization techniques. To tackle these two issues, a new model updating method is proposed to make full use of FRFs extracted from measured field data of structures and the improved particle swarm optimization (PSO) technique for accurately estimating physical parameters of structures. The novelties of this research include: (1) The signature assurance criterion (SAC)-based FRF is evaluated to eliminate the influence of limited frequency points on the accuracy of the updated model using the normalized acceleration component; (2) The enhanced PSO algorithm is developed to realize the adaptive selection of inertia factors for the better diversity by introducing an average value of the fitness function, and then accurate predictions of updating coefficients within a smaller number of iterations are achieved using the developed constraint factor. The effectiveness of the proposed method is verified by mathematical model of a jacket platform. Results show that the proposed method can accurately obtain the updating coefficients under spatial incomplete condition, and the maximum error of natural frequencies is 0.779% using the accelerations containing 5% noise. To prove the robustness of the proposed method, experimental studies of monopile offshore wind turbine are also conducted and the maximum error of natural frequencies is 1.887% under the consideration of spatial incompleteness represented by the structural stiffness degradation. Finally, the feasibility of the proposed method is evaluated by a test of a complex jacket platform, whose variation is

simulated by weakening the connections of some elements. The maximum error of natural frequencies predicted by the updated model is only 4.831% as compared with experimental results. Throughout these examples, the extended FRF model updating method provides engineers and designers with a useful insight into the development of reliable techniques to accurately predict dynamic responses of offshore structures.
Keywords: Model updating; Frequency response function; Signature assurance criterion; Normalized acceleration components; Improved particle swarm algorithm;

1. Introduction

Establishing a high-quality FE model is the basis for numerical analysis and performance state evaluation of offshore structures. However, due to the complexity of offshore structures and influences of the model order, structural parameter and type, there are still inevitable differences between the FE model and the actual structure. To reflect the actual operational state of offshore engineering structures, it is necessary to update and verify the FE model using the tested data.

At present, the common FE model updating methods can be divided into static and dynamic response-based methods according to types of structural responses (Mottershead et al., 1993). The FE model updating methods based on static responses were used to update the structure with more accurate static test data (such as displacement and strain). These data were measured in the structural test within the elastic range, to obtain a correct and reliable mathematical model for static analysis (Sanayei et al., 1997). Considering on the different updating parameters, there were two classes of methods: the matrix-based and the design parameter-based updating methods (Friswell et al., 1995). According to the different updating mechanism, the dynamic response-based FE model updating methods can be divided into two categories: modal parameter-based and frequency response function (FRF)-based model updating method (Zhang et al., 2023).

The modal parameter-based model updating methods have received extensive attention from scholars, along with the development of modal parameter identification techniques (Liu, 2011; Liu et al., 2013; Liu et al., 2016). Li et al. (2008) used the cross-model cross-mode (CMCM) method to simultaneously update the mass, damping and stiffness matrices of a FE model when

*Corresponding author.
Email address: percyliu@ouc.edu.cn (Fushun Liu)

Nomenclature			
a_1, a_2	Coefficients of Rayleigh damping	$MaxStep$	Number of maximum iteration
$\bar{a}_{rp}, \bar{a}_{rq}$	Amplitudes of pth and qth element in the rth acceleration component	N	Number of degrees of freedom
		$R(x)$	Objection function of improved particle swarm algorithm
$a_{j,noise}$	Noise-contaminated accelerations at the jth DOF	**SAC**	Signature assurance criterion of analytical and measured FRF
$\mathbf{C}, \mathbf{C}^*$	Damping matrices of analytical and measured system	$\mathbf{v}^0, \mathbf{x}^0$	Initial values of velocities and position for particles
C_1, C_2	Self-learning and social learning factors	$\mathbf{v}_{lim}, \mathbf{x}_{lim}$	Upper bound of velocities and position for particles
f_1, f_2	First-order and second-order natural frequencies	$\mathbf{y}, \dot{\mathbf{y}}, \ddot{\mathbf{y}}$	Displacement, velocity and acceleration of system
f_{ave}	Mean value of the fitness function	$\mathbf{Y}(\omega)$	Fourier transform of analytical displacement
f_g	Optimal fitness function value	α_n, β_n	Stiffness and mass variation coefficient of nth element
f_j	Fitness function value in jth iteration	ω_r	The rth natural frequency of the baseline model
$f, \mathbf{f}(\omega)$	Time and Fourier series of external loading	ω^*	Natural frequencies matrices of measured model
$\mathbf{g}_{best}, \mathbf{G}_{best}$	Local and global of optimal value for particle	$\varphi_{rp}, \varphi_{rq}$	Scalar values of rth mode at the pth and qth element
$\mathbf{H}(\omega), \mathbf{H}^*(\omega)$	FRF of analytical and measured system	ε	The level of noise
$\mathbf{K}, \mathbf{K}^*$	Stiffness matrices of analytical and measured system	δ	Random numbers in a Gaussian distribution
$\mathbf{M}, \mathbf{M}^*$	Mass matrices of analytical and measured system	δ_e	Error between the reconstructed and measured signal

only a few spatially incomplete complex-valued modes were available. Liu et al. (2014) proposed an improved modal strain energy method, which can identify the damage of jacket offshore wind turbines by defining a series of stiffness-updating factors. These factors can be used to calculate the modal strain energy of the measured structure without the consideration of the FE stiffness matrix. The above methods need to solve the equation to obtain the updating or damage coefficients of the structure. It should be noted that the ill-posed problem of solving equations is usually encountered. With the development of optimization algorithm, modal parameters were used to construct the relationship between the objective function and the updating parameters. Also and meta heuristic algorithm were applied to calculate the update coefficients, and overcome the ill-posed problem of solving equations (Tu et al., 2008; Begambre et al., 2009; Zhang et al., 2021). The objective function was usually composed of natural frequencies (Majumdar et al., 2012), mode shapes (Ngan et al., 2019) or their combinations (Bartilson et al., 2020). However, these parameters were not fully suitable to all types of structures in the model updating process. Results indicated that the population and iterations need to be increased when the complexity of the structure increases, leading to the increase the computational cost. Therefore, the computational efficiency of the algorithm was low, and the algorithm was easy to fall into local optimal solutions.

To improve the efficiency and accuracy of the optimization algorithm in calculating the structural updating parameters, the parameters that are sensitive to the location and extent of structural damage should be selected to construct the objective function. The model updating methods based on FRFs have been paid much attention due to several advantages (Jiang et al., 2014) including 1) FRFs are very sensitive to the damping of the structure at the resonance frequency peak, 2) the errors in the system identification are avoided as no modal analysis is required during the process of model updating and 3) the updating problem is over-determined due to the availability of FRFs at different excitation points. Modak et al. (2002) made a detailed comparison of the methods including inverse eigensensitivity and the response function for model updating in use of experimental data. The normal response function method was used to update the stiffness and mass matrices of the FE model and address the difficulties of updating the complex FRFs (Pradhan et al., 2012). Lin et al. (2006) updated the damping matrix of the structures using the FRFs to overcome the problem of complexity arising from measured FRFs and modal data. Lu et al. (2004) proposed a two-level neural network scheme for FE model updating and sensitivity analysis by a proper

response configuration. Esfandiari et al. (2009) used the frequency response function (FRF) and natural frequencies data for FE model updating, and the sensitivity equation normalization and proper selection of measured frequency points improved the accuracy and convergence in FE model updating. Arora et al. (2009a and 2009b) proposed a two-step procedure for updating the damping matrices and structural modifications with the reasonable accuracy and identified the damping matrix, and the normal frequency response functions (NFRFs) was proposed and tested with the objective that the damped FE model was able to predict the measured FRFs accurately using the normal FRFs (Arora et al., 2014). Canbaloğlu et al.(2016) used the pseudo receptance difference method to predict the linear FRFs from measured nonlinear FRFs, and the inverse eigensensitivity method was employed to update the linear FE model of the nonlinear structure. Hong et al.(2017) proposed a FRF-based model updating method, the method was formulated as an optimization problem which intended to minimize the difference between analytical and experimental FRF. However, the FRFs cannot be calculated accurately for the marine structures in service as it is impossible to achieve each order of modal parameter information. Therefore, errors will be introduced in the process of identifying the modal data, leading to the low calculation accuracy.

In this paper, a new model updating method based on extended FRFs and global optimization technique is proposed. Firstly, the complex exponential decomposition method is applied to extract the first several acceleration components, which are used to calculate the FRFs. Then the signature assurance criterion (SAC) is evaluated to eliminate the influence of limited frequency points and construct the objection function representing the first several natural frequencies. Finally, the updating coefficients are global optimized by the improved particle swarm optimization (PSO). Throughout three examples including mathematical model of a jacket platform, a physical monopile wind turbine and experimental tests of an offshore jacket platform, the effectiveness and feasibility of the proposed method are demonstrated for model updating of practical engineering structures.

2. Preliminaries

2.1. Frequency response function

The vibration equation for a linear multi-degree-of-freedom damped system is expressed as follows:

$$\mathbf{M}\ddot{\mathbf{y}} + \mathbf{C}\dot{\mathbf{y}} + \mathbf{K}\mathbf{y} = \mathbf{f} \tag{1}$$

where $\mathbf{M}$, $\mathbf{C}$ and $\mathbf{K} \in R^{N\times N}$ are the mass, damping and stiffness matrices of the system, respectively. $\mathbf{y}$, $\dot{\mathbf{y}}$ and $\ddot{\mathbf{y}} \in R^{N\times 1}$ depict the displacement, velocity and acceleration of the system. $\mathbf{f} \in R^{N\times 1}$ means the external loading, and N represents the number of degrees of freedom of the system.

Performing the Fourier transform on Eq. (1), the FRF of the system can be written as follows:

$$\mathbf{H}(\omega) = \frac{\mathbf{Y}(\omega)}{\mathbf{f}(\omega)} = \frac{1}{-\mathbf{M}\omega^2 + j\mathbf{C}\omega + \mathbf{K}} \tag{2}$$

where $\mathbf{Y}(\omega)$ and $\mathbf{F}(\omega)$ are the Fourier transforms of $\mathbf{y}$ and $\mathbf{f}$, respectively. ω represents the discrete frequency point in Hz and j is the imaginary number, i.e. $j^2 = -1$.

Ignoring the damping of system, the acceleration FRF $H_{pq}(\omega)$ representing the relationship between the load point q and the response point p can be expressed as follows:

$$H_{pq}(\omega) = \sum_{r=1}^{N} \frac{-\omega^2 \varphi_{rp}\varphi_{rq}}{\omega_r^2 - \omega^2} \tag{3}$$

where φ_{rp} and φ_{rq} are the scalar values of the rth mode at the element p and element q, respectively. ω_r means the rth natural frequency.

2.2. FRF-based objection function

For optimization-driven model updating methods the objection function is usually composed of design parameters including natural frequencies, mode shapes and the modal assurance criterion. Usually, these parameters are sensitive to the measurement noise and spatial incompleteness in practical engineering applications. Based on the frequency response function, the objection function based on FRF can be expressed as follows:

$$R(x) = \sum_{p=1}^{N}\sum_{q=1}^{N} \frac{|H_{pq}^*(\omega) - H_{pq}(\omega)|}{|H_{pq}(\omega)|} \tag{4}$$

where H_{pq}^* and H_{pq} represent the FRFs of the measured and baseline models, respectively. p and q depict the positions where the response and load are monitored.

3. The proposed model updating method

The governing equation of the measured model can be expressed as follows:

$$\mathbf{M}^*\ddot{\mathbf{y}}^* + \mathbf{C}^*\dot{\mathbf{y}}^* + \mathbf{K}^*\mathbf{y}^* = \mathbf{f} \tag{5}$$

where $\mathbf{y}^*$, $\dot{\mathbf{y}}^*$ and $\ddot{\mathbf{y}}^* \in R^{N\times 1}$ are the displacement, velocity and acceleration of the measured system, respectively. $\mathbf{K}^*, \mathbf{M}^*$ and $\mathbf{C}^*$ are the stiffness, mass and damping matrices of the measured model. To reflect the system change, $\mathbf{K}^*$ and $\mathbf{M}^*$ can be formulated as follows:

$$\mathbf{K}^* = \mathbf{K} + \sum_{n=1}^{N} \alpha_n \mathbf{K}_n;\ \mathbf{M}^* = \mathbf{M} + \sum_{n=1}^{N} \beta_n \mathbf{M}_n \tag{6}$$

where $\mathbf{K}_n$ and $\mathbf{M}_n$ are stiffness and mass matrices of the nth element, α_n and β_n denote the stiffness and mass variation coefficient of the nth element, respectively.

The FRF of the engineering structures can be measured directly in the dynamic test. As defined in Eq. (2), the FRF of the measured model is expressed as follows:

$$\mathbf{H}^*(\omega) = \frac{\mathbf{Y}^*(\omega)}{\mathbf{f}^*(\omega)} \tag{7}$$

Due to the influence of severe marine-environment and the limitations of sensors, it is difficult to accurately obtain the FRFs. However, the FRF $H^*_{pq}(\omega)$ of the measured model can be calculated using the modal superposition method:

$$H^*_{pq}(\omega) = \sum_{r=1}^{N} \frac{-\omega^2 \varphi^*_{rp}\varphi^*_{rq}}{\omega^{*2}_r - \omega^2} \tag{8}$$

Where φ^*_{rp} and φ^*_{rq} are the scalar values of the rth mode at elements p and q of the measured model, respectively. ω^*_r is the rth natural frequency of the measured model. Considering the influence of incomplete space, the Guyan method is used to match the degrees of freedom of FE model and actual structures. Only the low order modal parameters of the structure can be obtained in the actual. Combined with the research results (Esfandiari et al., 2009), when calculating the measured structure frequency response function, the high order modal parameters of the structure is replaced by the corresponding order modal parameters of the FE model.

$$H^*_{pq}(\omega) = \sum_{r=1}^{m} \frac{-\omega^2 \varphi^*_{rp}\varphi^*_{rq}}{\omega^{*2}_r - \omega^2} + \sum_{r=m+1}^{N} \frac{-\omega^2 \varphi_{rp}\varphi_{rq}}{\omega^2_r - \omega^2} \tag{9}$$

FRFs of the measured model can be obtained based on the relationship between the mode shapes and the acceleration components of the structure, which are extracted from the measured accelerations using the complex exponential method (Li et al., 2022). However, the accuracy of FRFs will be deteriorated as the modal identifying method introduces the secondary error. The acceleration FRF of the measured model can be re-written as:

$$H^*_{pq}(\omega) = \sum_{r=1}^{N} \frac{-\omega^2 \bar{a}_{rp}\bar{a}_{rq}}{\omega^{*2}_r - \omega^2} \tag{10}$$

where $\bar{a}_{rp}$ and $\bar{a}_{rq}$ represent the amplitudes of the pth and the qth elements in the rth normalized acceleration component, respectively.

To eliminate the effect of improper selection of frequency points on accuracy of updated model, the signature assurance criterion (SAC) of FRF H_{pq} for the structure is defined by Eq. (11):

$$SAC_{pq} = \frac{(|H_{pq}^{*t}(\omega)H_{pq}(\omega)|)^2}{[H_{pq}^{*t}(\omega)H_{pq}^{*}(\omega)][H_{pq}(\omega)^t H_{pq}(\omega)]} \tag{11}$$

where H_{pq}^{*} and H_{pq} are FRFs of the measured and baseline models, respectively, t indicates the transpose of the matrix. The SAC_{pq} is scaler, and the value of SAC range between 0∼1. It is noted that when SAC is equal to zero, it indicates that two FRFs are independent. When it is 1, they are completely correlated.

Substituting Eqs. (3) and (10) into Eq. (11), the SAC_{pq} can be rewritten as:

$$SAC_{pq} = \frac{[(\sum_{r=1}^{N} \frac{-\omega^2 \bar{a}_{rp}\bar{a}_{rq}}{\omega_r^{*2}-\omega^2})^t (\sum_{r=1}^{N} \frac{(-\omega^2 \varphi_{rp}\varphi_{rq})}{\omega_r^2-\omega^2})]^2}{[(\sum_{r=1}^{N} \frac{-\omega^2 \bar{a}_{rp}\bar{a}_{rq}}{\omega_r^{*2}-\omega^2})^t (\sum_{r=1}^{N} \frac{-\omega^2 \bar{a}_{rp}\bar{a}_{rq}}{\omega_r^{*2}-\omega^2})][(\sum_{r=1}^{N} \frac{-\omega^2 - \varphi_{rp}\varphi_{rq}}{\omega_r^2-\omega^2})^t (\sum_{r=1}^{N} \frac{-\omega^2 - \varphi_{rp}\varphi_{rq}}{\omega_r^2-\omega^2})]} \tag{12}$$

Considering the effect of FRFs on the accuracy of the updated model, the matrix **SAC** can be expressed as follows:

$$\mathbf{SAC} = \frac{[\mathbf{H}^{*t}(\omega)\mathbf{H}(\omega)]^2}{[\mathbf{H}^{*t}(\omega)\mathbf{H}^{*}(\omega)][\mathbf{H}^{t}(\omega)\mathbf{H}(\omega)]} = \frac{[-\omega^2\mathbf{M}^{*}+\mathbf{K}^{*}](-\omega^2\mathbf{M}+\mathbf{K})^t}{(-\omega^2\mathbf{M}+\mathbf{K})[-\omega^2\mathbf{M}^{*}+\mathbf{K}^{*}]^t} \tag{13}$$

where $\mathbf{H}^{*}$ and $\mathbf{H}$ are the matrices of FRFs for the measured and baseline model, respectively.

Employing the eigenvalue-analysis method, the natural frequencies of the measured and baseline models can be obtained by Eq. (14):

$$\omega^{*} = \sqrt{\mathbf{K}^{*}/\mathbf{M}^{*}},\ \omega = \sqrt{\mathbf{K}/\mathbf{M}} \tag{14}$$

where ω^{*} and ω are the matrices of natural frequencies for measured and baseline models, respectively.

Therefore, the objection function can be constructed using the natural frequencies and SAC in the form of Eq. (15):

$$\begin{aligned}\mathbf{R}(x) = &\frac{|\sqrt{\mathbf{K}\mathbf{M}^{-1}} - \sqrt{\mathbf{K}(\mathbf{I}+\alpha)[\mathbf{M}(\mathbf{I}+\beta)]^{-1}}|}{\sqrt{\mathbf{K}(\mathbf{I}+\alpha)[\mathbf{M}(\mathbf{I}+\beta)]^{-1}}} \\ &+ \left\{\mathbf{I} - \frac{[-\omega^2\mathbf{M}(\mathbf{I}+\beta)+\mathbf{K}(\mathbf{I}+\alpha)](-\omega^2\mathbf{M}+\mathbf{K})^t}{(-\omega^2\mathbf{M}+\mathbf{K})[-\omega^2\mathbf{M}(\mathbf{I}+\beta)+\mathbf{K}(\mathbf{I}+\alpha)]^t}\right\}\end{aligned} \tag{15}$$

where $\alpha, \beta \in R^{N\times 1}$ are the variation coefficients of structural stiffness and mass matrices, respectively.

It is noted that Eq. (15) can also be formulated as:

$$\mathbf{R}(x) = \frac{|\sqrt{\mathbf{K}\mathbf{M}^{-1}} - \sqrt{\mathbf{K}\Lambda(\mathbf{M}\Gamma)^{-1}}|}{\sqrt{\mathbf{K}\Lambda(\mathbf{M}\Gamma)^{-1}}} + \left[\mathbf{I} - \frac{(-\omega^2\mathbf{M}\Gamma + \mathbf{K}\Lambda)(-\omega^2\mathbf{M} + \mathbf{K})^t}{(-\omega^2\mathbf{M} + \mathbf{K})(-\omega^2\mathbf{M}\Gamma + \mathbf{K}\Lambda)^t}\right] \tag{16}$$

where $\Lambda = \mathbf{I} + \alpha$ and $\Gamma = \mathbf{I} + \beta$.

3.1. Global optimization of the updating coefficients

The optimal updating coefficients α and β of the structure can be obtained using the improved particle swarm optimization (IPSO) algorithm. The initial parameters of the IPSO algorithm are set by Eq. (17).

$$\begin{aligned} &\mathbf{x}^0 = \left\{\alpha_1^0, \alpha_2^0, \cdots, \alpha_n^0, \beta_1^0, \beta_2^0, \cdots, \beta_n^0\right\};\ MaxStep \\ &\mathbf{v}^0 = \left\{v_1^0, v_2^0, \cdots, v_{2n}^0\right\};\ \mathbf{x}_{lim} = \{x_l; x_u\};\ \mathbf{v}_{lim} = \{v_l; v_u\} \end{aligned} \tag{17}$$

where $\mathbf{x}^0$ and $\mathbf{v}^0 \in R^{m\times 2n}$ are the initial values of the updating coefficients and velocities for particles, respectively. $\mathbf{x}_{lim}, \mathbf{v}_{lim} \in R^{2\times 2n}$ are the upper bound of the updating coefficients and velocities for particles. $MaxStep$ is the number of maximum iterations.

Using the acceleration components of the measured model and modal data of the baseline model, the objection function can be evaluated for the local and global optimum by Eq. (18)

$$\mathbf{g}^0 = \mathbf{g}_{best}^0;\ \mathbf{G}^0 = \mathbf{G}_{best}^0; \tag{18}$$

where $\mathbf{g}^0, \mathbf{G}^0 \in R^{1\times 2n}$ are the local and global optima for the initial particles in the IPSO algorithm.

The expressions of the velocity $\mathbf{v}$ and position $\mathbf{x}$ of particles in the $j+1$th iteration can be expressed as follows:

$$\mathbf{v}^{j+1} = \chi \times [\widehat{\omega} \times \mathbf{v}^j + C_1 \times rand \times (\mathbf{g}_{best}^j - \mathbf{x}^j) + C_2 \times rand \times (\mathbf{G}_{best}^j - \mathbf{x}^j)] \tag{19}$$

$$\mathbf{x}^{j+1} = \mathbf{x}^j + \mathbf{v}^{j+1} \tag{20}$$

where C_1 and C_2 are the self-learning and social learning factors, respectively, i.e. $C_1 = C_2 = 2$. $rand$ denotes the random number between 0 and 1. $\mathbf{g}_{best}^j$ and $\mathbf{G}_{best}^j \in R^{1\times 2n}$ denote the local and global optima of the particles at the jth iteration. m represents the population of particles. The constrain factor χ and the adaptive inertia factor $\widehat{\omega}$ can be further defined by Eqs. (21) and (22).

$$\chi = (\cos(\pi * j/MaxStep) + 2.5)/4 \tag{21}$$

$$\hat{\omega} = \begin{cases} \omega_{max} - (\omega_{max} - \omega_{min}) \times \left| \frac{f_j - f'_{ave}}{f_g - f'_{ave}} \right|; \ f_j \leqslant f'_{ave} \\ \omega_{min} + (\omega_{max} - \omega_{min}) \times \frac{1+cos((j-1)\pi/(MaxStep-1))}{2}; \ f'_{ave} \leq f_j \leqslant f_{ave} \\ 1.5 - \frac{1}{1+k_1 \cdot exp(-k_2) \cdot \Delta}; \ f_j > f_{ave} \end{cases} \tag{22}$$

where ω_{max} and ω_{min} are the maximum and minimum values of the inertia factor, respectively, e.g. $\omega_{max} = 0.9$ and $\omega_{min} = 0.4$, f_{ave} represents the mean value of the fitness function, and f'_{ave} stores the better value of f_{ave}. f_g is the optimal fitness function value and f_j is the fitness function value in the jth iteration. $\Delta(\Delta = \left| f_g - f'_{ave} \right|)$ is used to evaluate the early convergence of the particle, $k_1 = 1.5$ and $k_2 > 0$.

In the $j+1$th iteration, the local and global optimal value are updated by Eqs. (23) and (24).

$$\mathbf{g}_{best}^{j+1} = \begin{cases} \mathbf{x}^{j+1}; & R(\mathbf{x}^{j+1}) \leqslant R(\mathbf{g}_{best}^{j}) \\ \mathbf{g}_{best}^{j}; & R(\mathbf{x}^{j+1}) > R(\mathbf{g}_{best}^{j}) \end{cases} \tag{23}$$

$$\mathbf{G}_{best}^{j+1} = \begin{cases} \mathbf{g}_{best}^{j+1}; & R(\mathbf{g}_{best}^{j+1}) \leqslant R(\mathbf{G}_{best}^{j}) \\ \mathbf{G}_{best}^{j}; & R(\mathbf{g}_{best}^{j+1}) > R(\mathbf{G}_{best}^{j}) \end{cases} \tag{24}$$

When the algorithm satisfies the termination criteria, the global optimal of the updating coefficients is achieved by Eq. (25).

$$\begin{aligned} \mathbf{G}_{best} &= \{\alpha_1, \alpha_2, \cdots, \alpha_n, \beta_1, \beta_2, \cdots, \beta_n\} \\ &= min \left\{ \frac{|\sqrt{\mathbf{K}\mathbf{M}^{-1}} - \sqrt{\mathbf{K}\Lambda(\mathbf{M}\Gamma)^{-1}}|}{\sqrt{\mathbf{K}\Lambda(\mathbf{M}\Gamma)^{-1}}} + \left[\mathbf{I} - \frac{(-\omega^2\mathbf{M}\Gamma + \mathbf{K}\Lambda)(-\omega^2\mathbf{M} + \mathbf{K})^t}{(-\omega^2\mathbf{M} + \mathbf{K})(-\omega^2\mathbf{M}\Gamma + \mathbf{K}\Lambda)^t} \right] \right\} \end{aligned} \tag{25}$$

where the $\mathbf{G}_{best}$ is the global optimum after the iterative operation of the improved PSO through minimizing the objection function for each iteration.

3.2. The process of the proposed method

The flowchart of the proposed method is shown in Fig. 1, and the procedure of the proposed method for model updating is described as follows:

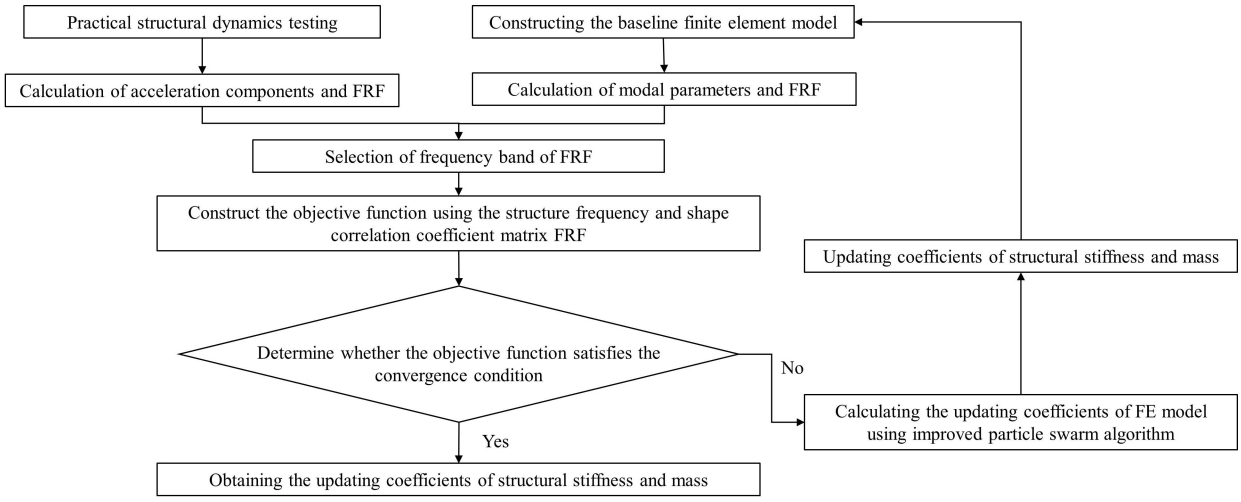

Fig. 1: Numerical example of jacket platform structure

Step 1: Using the complex exponential decomposition method, the normalized acceleration components of the measured model can be obtained, then FRFs of baseline and measured models can be calculated according to Eqs. (3) and (10).

Step 2: Based on the FRFs of baseline and measured models, SAC is calculated by Eq. (12). Following that, the objection function formulated by Eq. (15) can be constructed for calculation of the updating coefficients, given SAC and the natural frequencies.

Step 3: Initializing the parameters of the IPSO algorithm using Eq. (17), the updating coefficients of structural stiffness and mass can be achieved according to Eqs. (18)∼(25).

4. Numerical example of jacket platform structure

To verify the effectiveness of the proposed method, a numerical study of a jacket platform shown in Fig. 2, is carried out. The model consists of 46 steel pipe members, including 12 vertical bracing members with 0.9 m diameter and 0.03 m wall thickness, 22 cross bracing members with 0.6 m diameter and 0.02 m wall thickness, and 12 diagonal bracing members with 0.3 m diameter and 0.018 m wall thickness. The elevations of the structure from bottom to top are -2.00 m, 3.00 m, and 8.50 m. The top side lengths are 11.00 m, 8.10 m, 11.00 m, and 8.10 m, and the bottom side lengths are 12.45 m, 9.20 m, 12.45 m, and 9.20 m. The specific details are shown in Table 1.

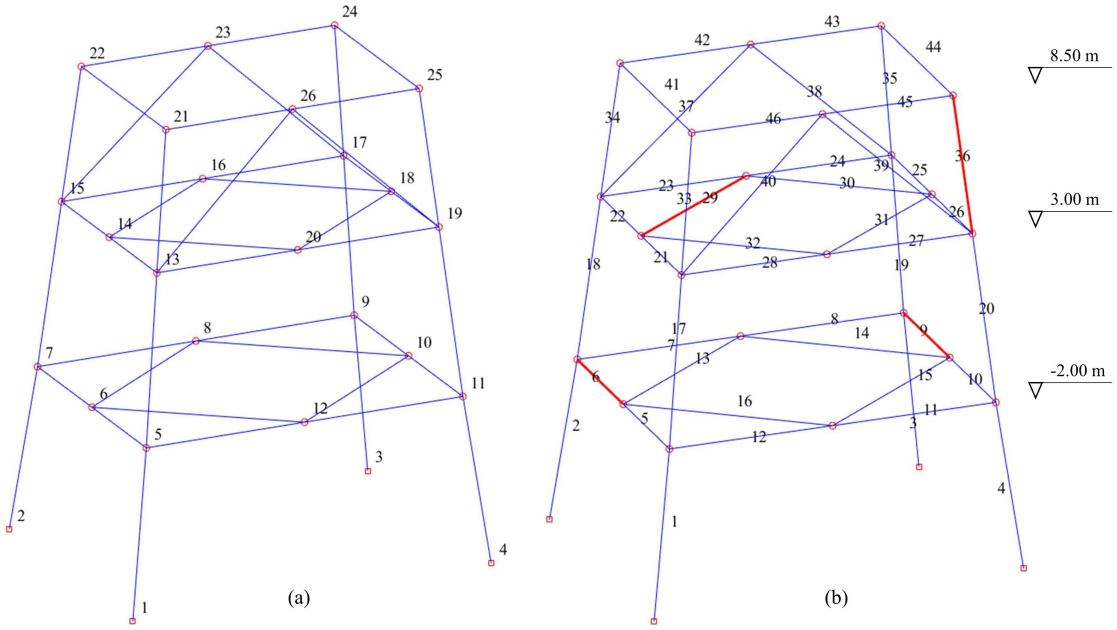

Fig. 2: Numerical example of jacket platform structure (a) Number of node (b) Number of element

Table 1: Parameters of the numerical model of the jacket platform

Type of element	Diameter (m)	Wall thickness (m)
Vertical bracing	0.9	0.03
Cross bracing	0.6	0.02
Diagonal bracing	0.3	0.018

The numerical model of the jacket platform is constructed using MATLAB software, and its material properties include the modulus of elasticity the modulus of elasticity of 210 Gpa, the density of 7850 kg/m^3, the Poisson's ratio of 0.3. The model has 43 elements and 26 nodes, each of node has 3 translational degrees of freedom and 3 rotational degrees of freedom. All degrees of freedom of the nodes in contact with the ground are full constrained, i.e., Nodes 1 to 4.

To simulate the changes in vibration characteristics of the jacket platform during service, it is assumed that the stiffness and mass of the red line segment of the model shown in Fig. 2 can

be changed, and its damping parameters are kept constant. The stiffness degradation coefficients areα_6 = -0.4, α_9 = -0.25, α_{29} = -0.35 and α_{36} = -0.3, and the mass variation coefficients are β_6 = 0.3, β_9 = 0.5., β_{29} = 0.2 and β_{36} = 0.15. Also, Fluent is used in the analysis and the Jonswap spectrum (Hasselmann et al., 1973) is applied to simulate the wave surface with a peak period of 5 s and a significant wave height of 0.25 m. The water surface height is 8 m.

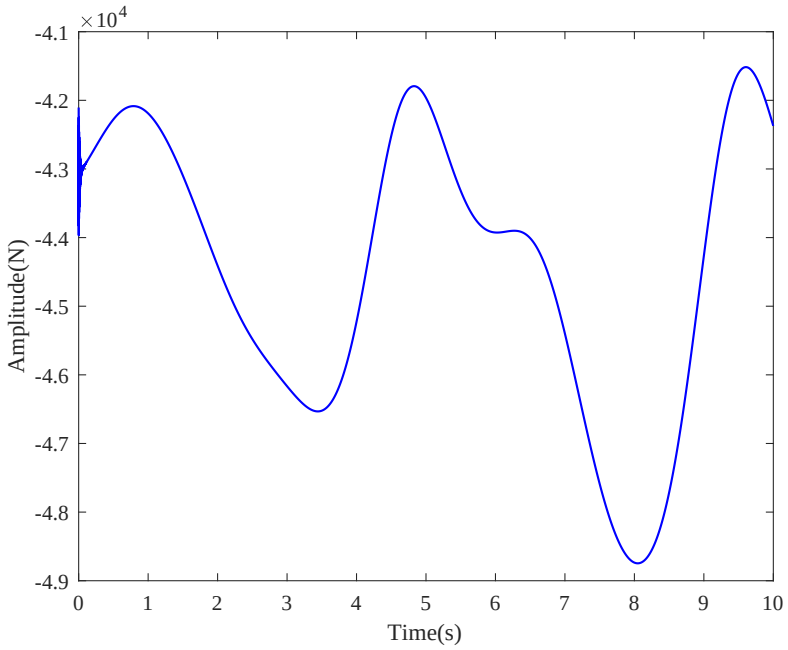

Fig. 3: Time curve of the wave load

The wave load is applied to the jacket platform model in the form of equivalent nodal force, and the load magnitude of the nodal degrees of freedom above the water surface is 0. The duration of the load is 10 s, and the sampling time interval is 0.001 s. Taking the degree of freedom of Node 5 as an example, the time curve of the wave load acting on it is shown in Fig. 3. Dynamic responses of the system are calculated using the Newmark-β method. To demonstrate the performance of the proposed method, the incomplete accelerations with the measurement noise are used to calculate the updating coefficients of the system.

4.1. Model updating using the incomplete accelerations

It is challenging to arrange sensors on the jacket platform below the water surface due to the environmental conditions, and accurately obtain the responses regarding structural rotations.

Therefore, the influence of spatial incompleteness needs to be considered in the model updating study of marine engineering structures. To simulate the effects of spatial incompleteness conditions in actual marine structures, it is assumed that only the acceleration responses of Nodes 13-26 in the X, Y and Z translational can be obtained. The measured acceleration response are decomposed and reconstructed using the complex exponential decomposition method. Taking the degrees of freedom of Nodes 13, 15, 17 and 19 as an example, and the results are shown in Fig. 4.

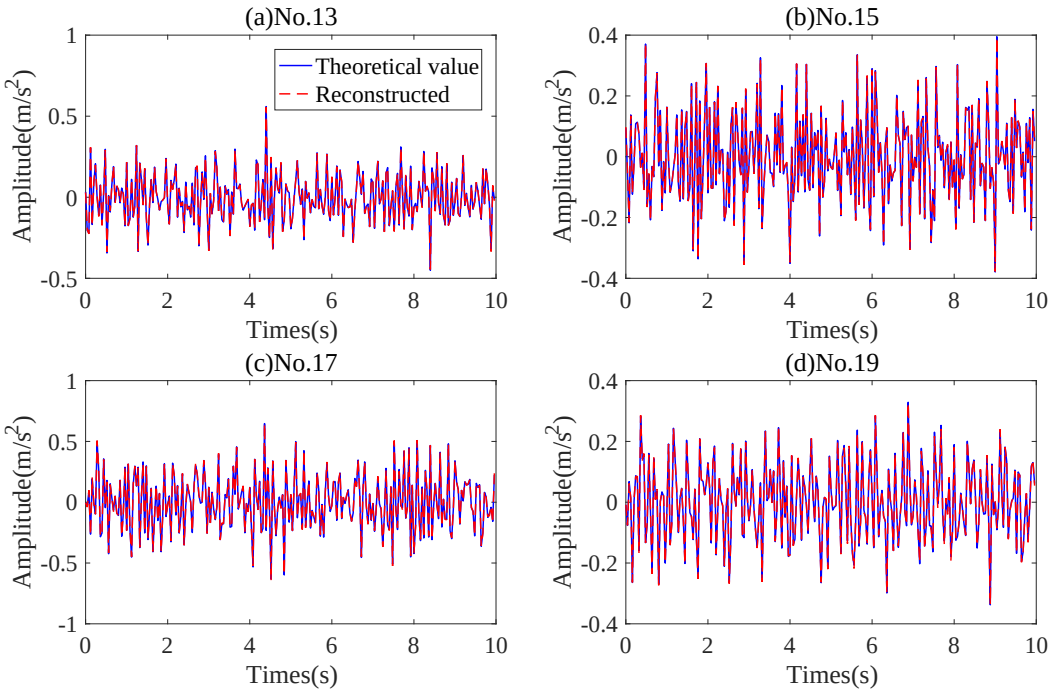

Fig. 4: Reconstructed acceleration signals of jacket platform

It is noted that the reconstruction results completely agree with the theoretical values from Fig. 4, verifying the effectiveness of the proposed method. To quantify the computational accuracy of the complex exponential decomposition method, the error between the reconstructed and theoretical signal is calculated, and the formula can be written as follows:

$$\delta_e(t) = a_r(t) - a_m(t) \tag{26}$$

where $a_r(t)$ and $a_m(t)$ represent the reconstructed and theoretical acceleration, respectively.

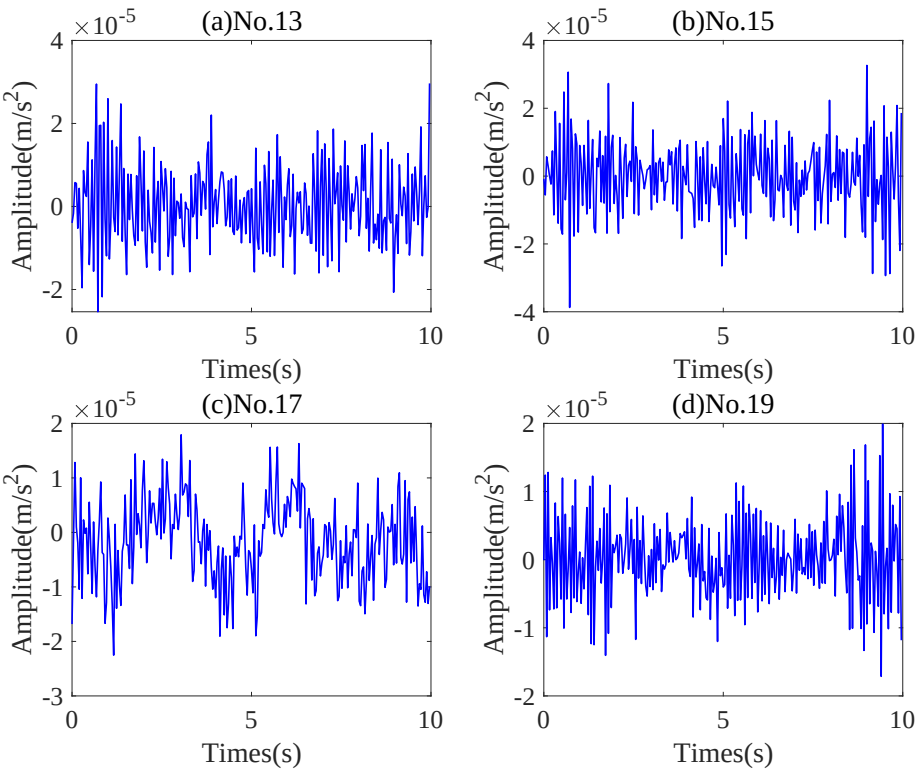

Fig. 5: Error curve between the reconstructed and theoretical signal

The error curve between the reconstructed and theoretical signal is shown in Fig. 5 and it can be observed that the maximum errors of 4 nodes are 3.701×10^{-5}, 3.862×10^{-5}, 1.454×10^{-5} and 3.334×10^{-5}, respectively. This indicates the effectiveness of proposed method for decomposing and reconstructing signal. The acceleration components corresponding to the first three natural frequencies of the structure are extracted from results by the complex exponential component method. Again, taking the degrees of freedom of Nodes 13, 15, 17 and 19 as an example, and the time curves of acceleration components of the structure are shown in Fig. 6. The structural acceleration components and frequency response function can be further obtained using the amplitudes at different times and Eq. (10), respectively. In Fig. 7, H_{11}, H_{12}, H_{13} and H_{14} are shown for numerical jacket platform model. It can be observed that the difference of frequency response functions between the baseline and the measured model is noticeably large.

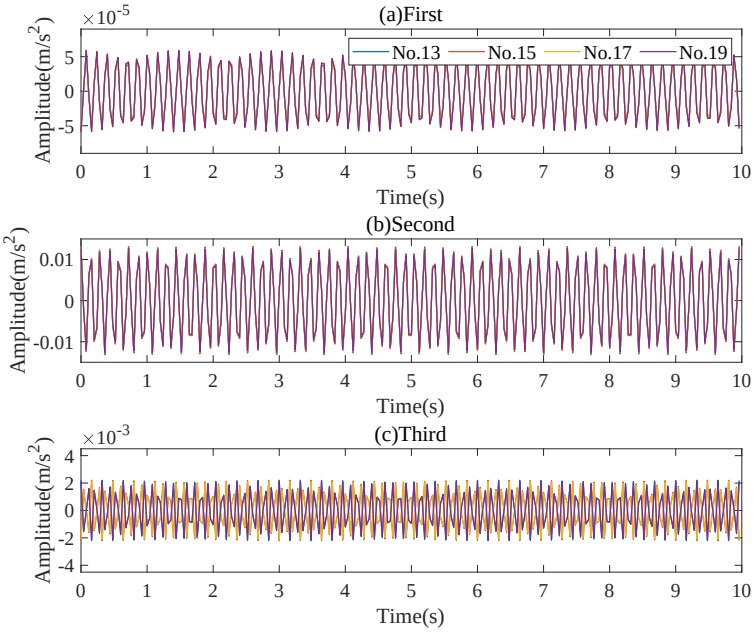

Fig. 6: Time curve of the first three acceleration components

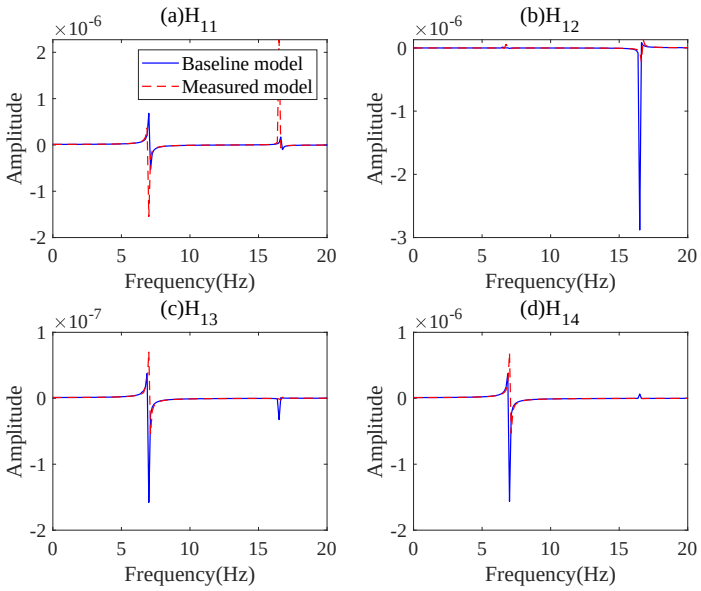

Fig. 7: Frequency response function of numerical jacket platform model

The first three modal parameters of the jacket platform during the service time can be numer-

ically obtained. To select the appropriate frequency range of frequency response functions for the calculation of updating coefficients, the different frequency range is determined according to the structural acceleration spectrum. Taking Node 13 as an example, the detailed frequency range is shown in Fig. 8.

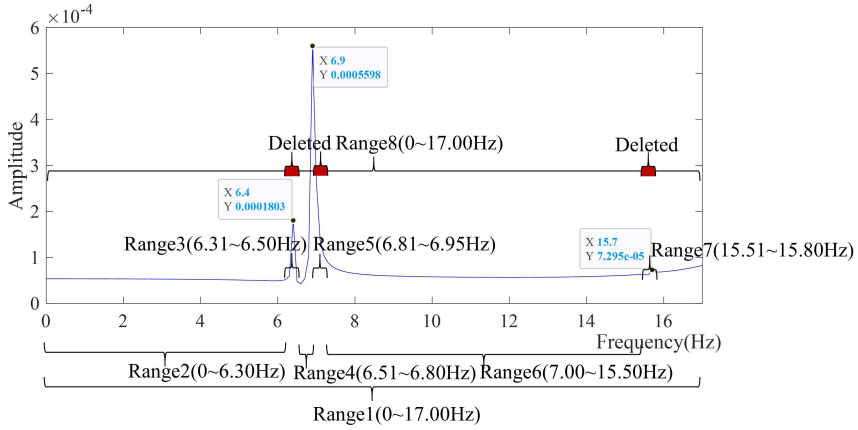

Fig. 8: Division of frequency range

To weaken the influence of the frequency range selection on the updating results, the SAC for adjacent degrees of freedom at different frequency ranges is calculated and its result is shown in Fig. 9. It can be observed that the average SAC values of the Ranges 6 and 8 are smaller, indicating that the FRF of these two frequency ranges are more sensitive to the variation of structural characteristics. To reduce the computational cost of updating coefficients, the range 6 is chosen to calculate the matrices of SAC in the numerical jacket platform model. In the Fig. 10, SAC values of the complete and incomplete FRFs are provided, respectively. Total 90 parameters are included in the incomplete FRF, while the complete FRF has more parameters. As the gap between the baseline model and the measured structure can not be highlighted, the structural complete FRF is applied in the following analysis.

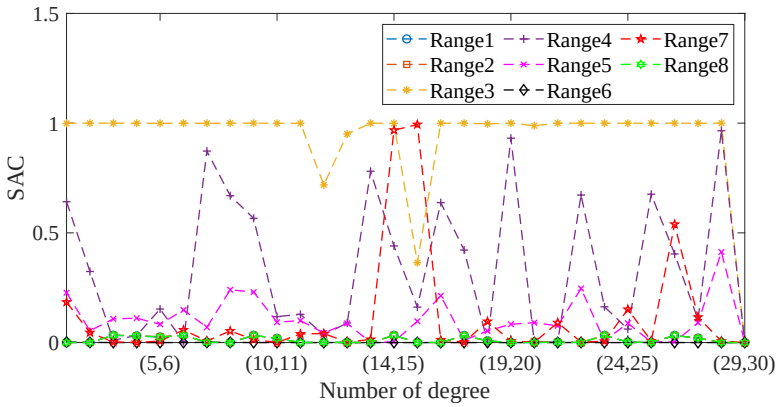

Fig. 9: Division of frequency range for numerical jacket platform model

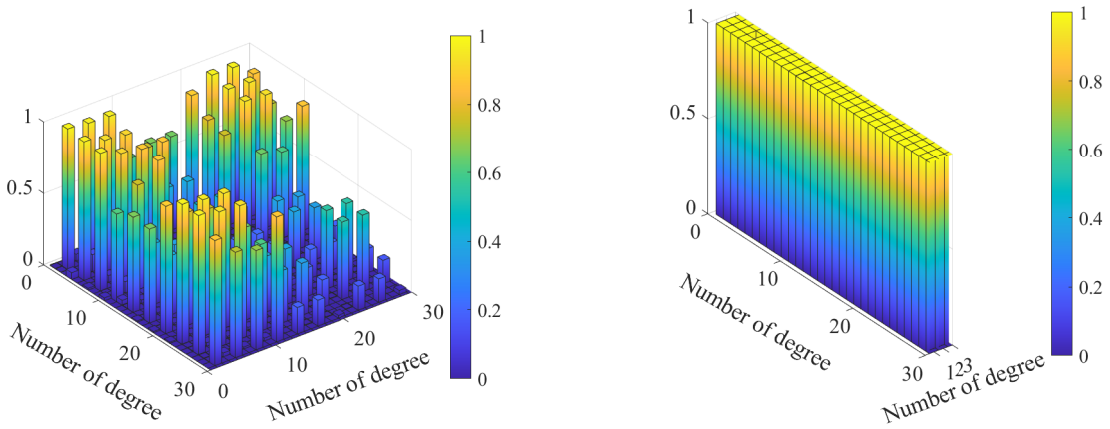

Fig. 10: SAC of :(a) Complete FRF; (b) Incomplete FRF

The jacket platform is modeled with 46 elements and there are 92 updating coefficients to be calculated in the updating process of the structural stiffness and mass. The incomplete FRFs can only provide 87 SACs, which are insufficient to construct the objective function. According to the calculation process described in Section 3.2, the objective function is constructed by applying the SACs of the complete FRFs shown in Fig. 10(a) and the first three natural frequencies by Eq. (16). The population and generation in the improved particle swarm algorithm are defined as 1000 and 100, respectively. The fitness function curve and the updating coefficients are shown in Fig. 11 and Fig. 12, respectively.

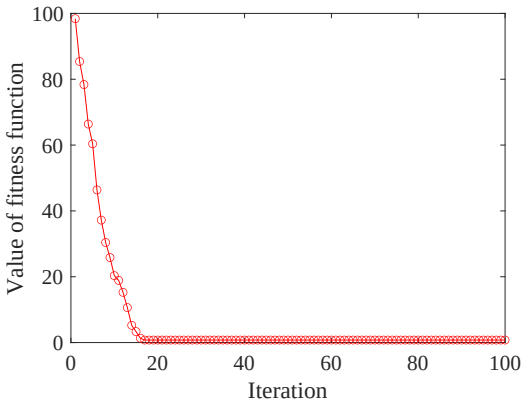

Fig. 11: Convergence curve of fitness function

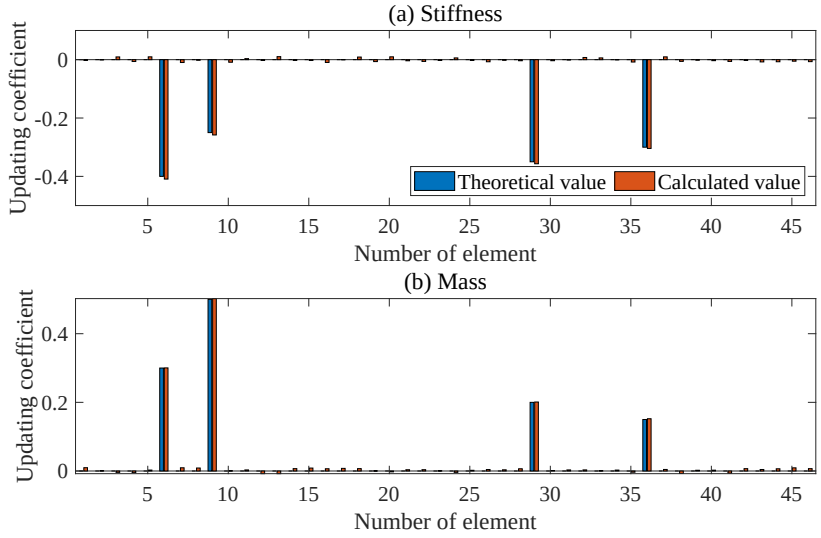

Fig. 12: Result of updating coefficients

Based on the convergence curve in Fig. 11, it can be noted that the improved particle swarm algorithm converges to the global optimal value after about 20 cycles, which verifies the effectiveness of the improved particle swarm algorithm. As compared with the theoretical values, the calculated coefficients shown in Fig. 12 demonstrate a good accuracy. To further evaluate the agreement between the updated model and the actual structure, the natural frequencies of the updated model in Table 2 are calculated using the eigenvalue-method. It is concluded that the maximum error of the first three natural frequencies is 0.249%, which meets the requirement of the model updating accuracy and verifies the correctness of the proposed method.

Table 2: The natural frequencies of updated numerical jacket platform model

n	Theoretical value	Baseline model	Error(%)	Updated model	Error(%)
1	6.421	6.737	4.921	6.405	0.249
2	6.928	7.055	1.833	6.920	0.115
3	15.664	16.671	6.428	15.647	0.109

4.2. Model updating using the noise-contaminated accelerations

To investigate the effect of the measurement noise, a series of random numbers are added to the acceleration signals to represent the noise:

$$a_{j,noise} = a_j(1 + \delta\varepsilon) \tag{27}$$

where a_j is the acceleration at jth DOF of the structure; δ is a random numbers in a Gaussian distribution with a mean value of 0 and a standard deviation of 1; and ε indicates the noise level, which is defined in the set (0.5%, 1%, 5%).

The acceleration signals of the structure at nodes 13, 15, 17 and 19 under different noise conditions are shown in Fig. 13. Based on the calculation process in Section 3.2, the structural acceleration responses are decomposed and reconstructed using the complex exponential decomposition method. The reconstructed acceleration signals containing 5% noise at those nodes along the translational direction are provided in Fig. 14. The error between the reconstructed and theoretical value can be calculated by Eq.(26), and the maximum errors of different nodes are 8.521×10^{-3}, 7.201×10^{-3}, 1.112×10^{-2} and 1.125×10^{-2}, respectively. It can be concluded that the reconstructed results well agree with the original signals, indicating that the complex exponential decomposition method can accurately achieve the decomposition and reconstruction of the acceleration responses and also demonstrate the effectiveness of the proposed method with the denoising capability.

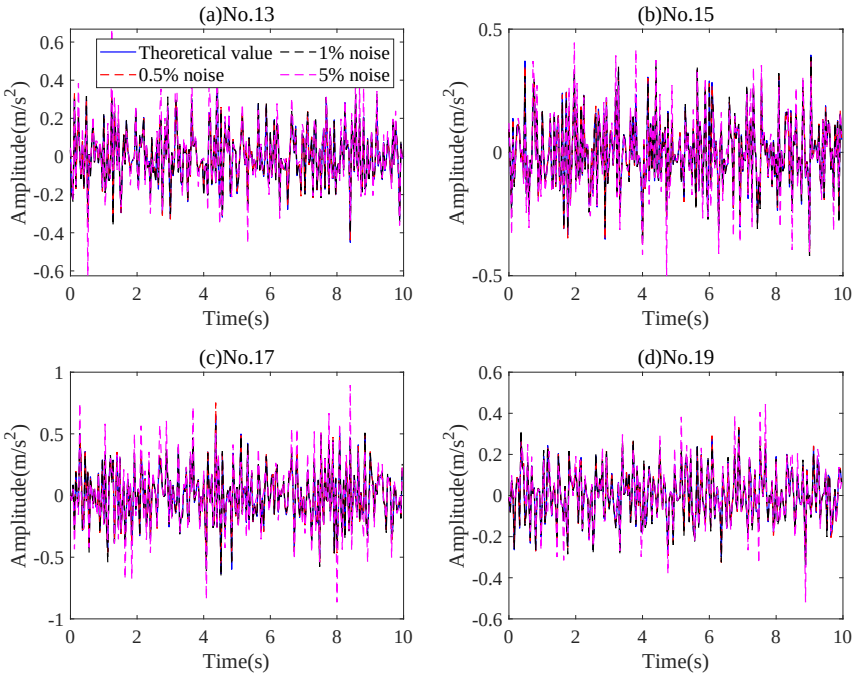

Fig. 13: Time curve of the acceleration signals under different noise

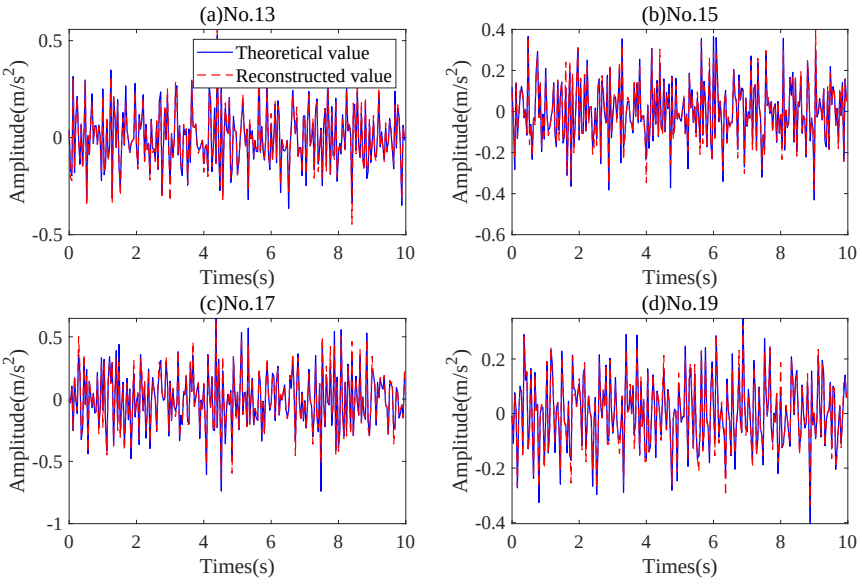

Fig. 14: Reconstructed acceleration signals under 5% noise

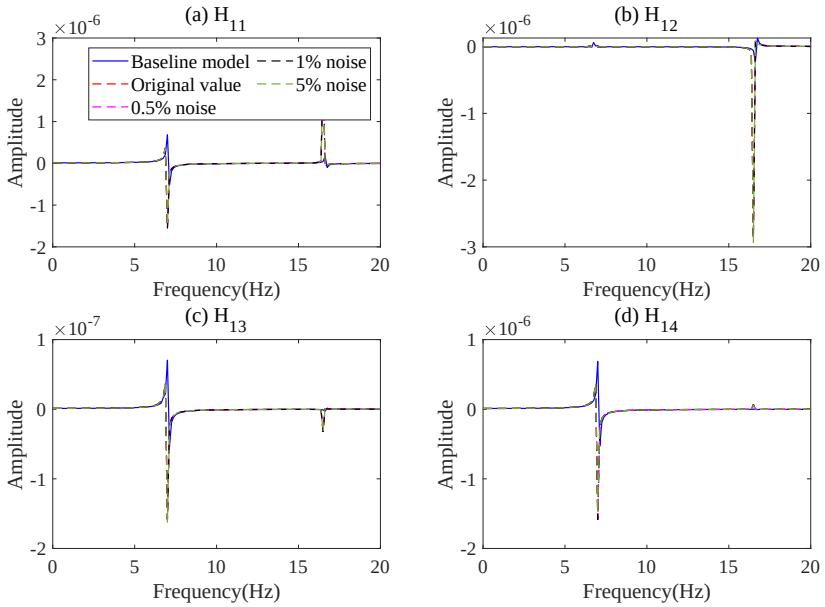

Fig. 15: FRF of jacket platform under different noise

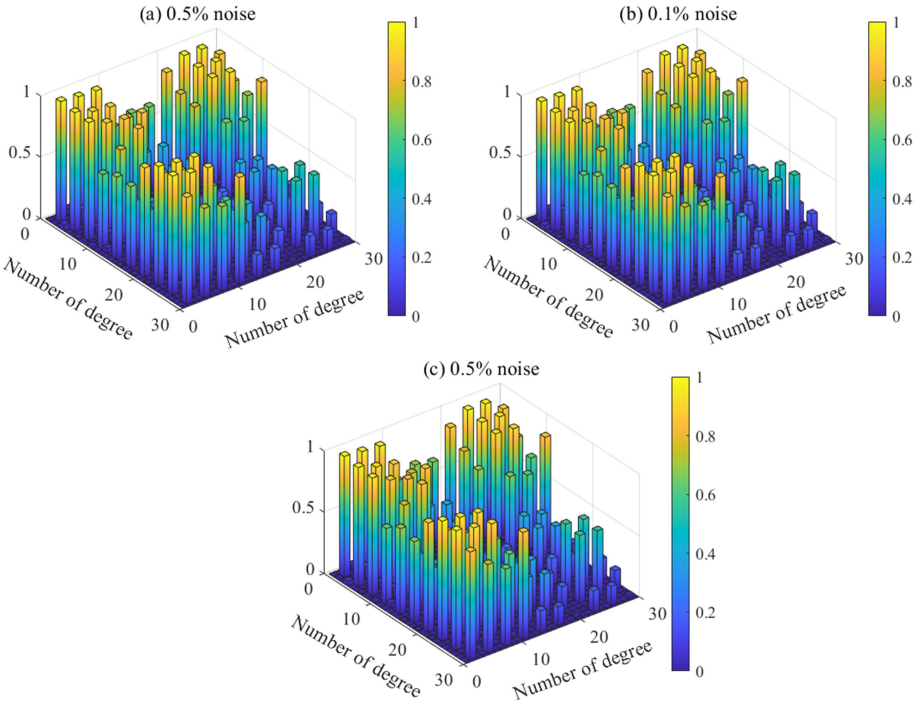

Fig. 16: SACs of jacket platform under different noise

The complete FRFs of the jacket platform under different level noise conditions are calculated

according to Eq. (10). Results labelled as H_{11}, H_{12}, H_{13} and H_{14} are shown in Fig. 15. It is worth noting that the amplitude of the FRF does not change with the increase of the noise level, indicating that the FRF is not sensitive to noise. Using the data of range 6, the SACs of complete FRFs are shown in Fig. 16. The maximum values of SAC are 0.984, 0.984 and 0.979, which enable the construction of the objection function for the optimal updating coefficients of offshore structures using the improved particle swarm optimization technique.The fitness function and updating coefficients under different levels of noise conditions are shown in Fig. 17 and Fig. 18, respectively.

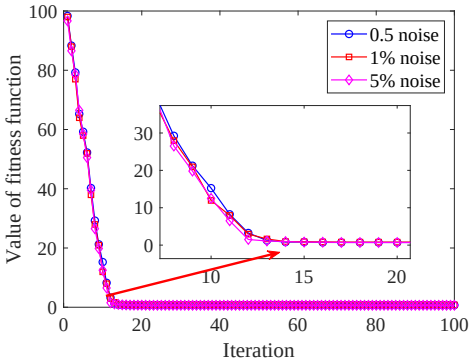

Fig. 17: Convergence curve of fitness function under different levels of noise

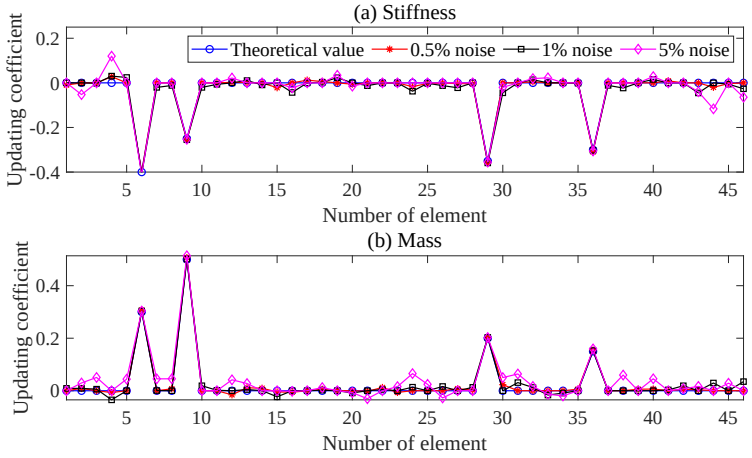

Fig. 18: Updating coefficients of jacket platform under different levels of noise

To further evaluate the degree of matching between the updated model and the actual structure, the natural frequencies updated model are calculated, and the results are listed in Table

3. According to the data in the Table 3, it can be observed that the maximum error of natural frequencies between the updated model and the theoretical value is 0.779%, indicating that the proposed model updating method in this paper has better robustness and accuracy considering the effect of spatial incompleteness and noise.

Table 3: The natural frequencies of updated model under different noise levels

n	Theoretical value	0.5% noise	Error(%)	1% noise	Error(%)	5% noise	Error(%)
1	6.421	6.403	0.280	6.402	0.296	6.380	0.639
2	6.928	6.912	0.231	6.907	0.303	6.906	0.318
3	15.664	15.631	0.211	15.631	0.211	15.542	0.779

5. Experimental study on monopile wind turbine

To verify the performance of the proposed method in practical engineering applications, an experimental study of a monopile wind turbine model is carried out in the Vibration Laboratory at the Ocean University of China. The model is fully fixed on the vibration platform in the experiment, while the harmonic load is applied on the top of the model using the eccentric rotating device. Seven accelerometers and two displacement sensors are mounted on the model to measure the acceleration and displacement responses, respectively.

5.1. Experiment setup

The model consists of four parts: the foundation, connecting flange, tower and the nacelle. The foundation is made from circular steel tubes with a height of 900 mm, a wall thickness of 2.2 mm and an out diameter of 96 mm. The diameter of flange is 196 mm, which is connected by 12 bolts. The tower is composed of variable cross-section steel tubes with the height of 1200 mm, a wall thickness of 2.2 mm, and a diameter in range of 50 to 90 mm from top to bottom. The nacelle is made from light composite materials. The elastic modulus of the steel tube is 210 GPa with the density is 7850 kg/m^3 and the Poisson's ratio of 0.3.

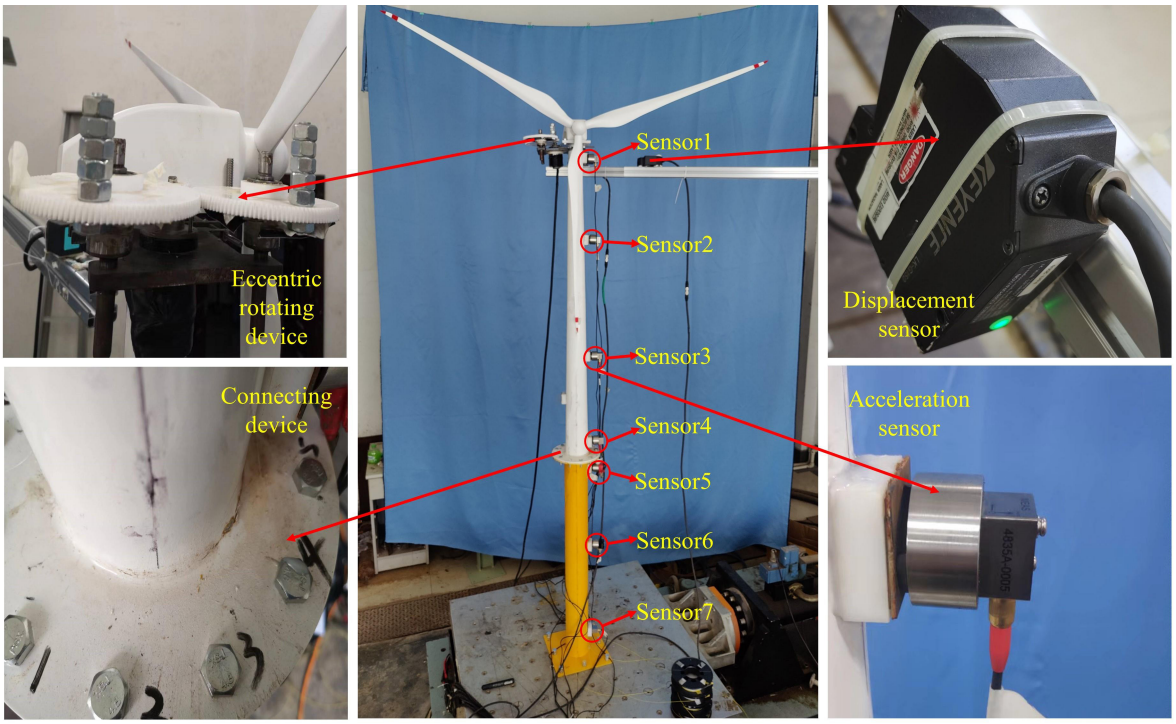

Fig. 19: The diagram of the experiment for monopile wind turbine

The eccentric rotation device is installed at a distance of 20 mm from the top of the model, and its mass is 1.98 kg. Also, a sinusoidale loading of 10.285 N with a period of 0.176 s is applied on the model and this load is simulated by the spinning device with a rotational speed of 340 rpm. The seven accelerometers are positioned at the distance of 50 mm, 500 mm, 850 mm, 950 mm, 1300 mm, 1700 mm and 2050 mm measured from the top of the model are labelled as Sensor1∼Sensor7. The positions of laser displacement sensors (Sensor8 and Sensor9) correspond to the X and Y directions of the Sensor1. The acceleration and displacement signals are recorded by the CRONOS CRFX-400 with a sampling frequency of 200 Hz , and the diagram of the experiment is shown in Fig. 19.

5.2. Description of the baseline model

The monopile wind turbine is modelled with two-node beam elements using MATLAB to match the degrees of freedom between the FE model and the measured structure. The lengths of each cell from top to bottom are 100 mm, 400 mm, 350 mm, 100 mm, 350 mm, 450 mm and 350 mm, respectively. To simplify the calculation of the subsequent updating coefficients, the modeling

process does not consider the effect of the boundary conditions at the connection between the tower and the foundation. Also, the stiffness degradation at the connection is represented by the discounted equivalent stiffness of the element. It is assumed that only the mass and stiffness matrices of the wind turbine need to be updated. Using the eigenvalue-analysis method, the first two mode shapes of the FE model are shown in Fig. 20, and the corresponding first two natural frequencies are 9.222 Hz and 42.334 Hz, respectively.

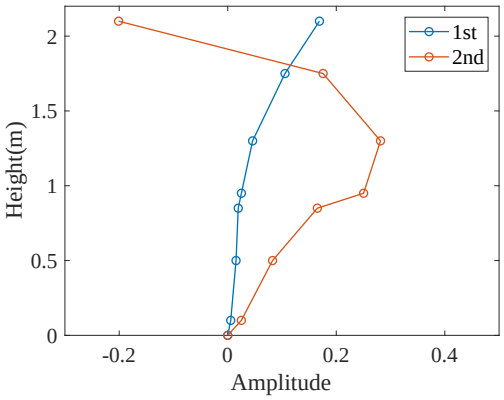

Fig. 20: Modal shape of the wind turbine model

5.3. Load and working condition settings

To simulate the stiffness degradation of the flange in the experiment, four cases are considered by removing different numbers of bolts shown in Table 4. The diagram of bolts at the flange in the four cases is shown in Fig. 21. As the accurate damping characteristics of complex structures can hardly predicted in practical engineering, it is assumed that the damping of the structure keeps constant, and only the mass and stiffness of the structure need to be updated. The damping matrix is usually calculated using the Rayleigh damping model(Craig and Kurdila, 2006), which can be expressed as follows:

$$\mathbf{C} = a_1\mathbf{M} + a_2\mathbf{K} \tag{28}$$

$$\begin{pmatrix} a_1 \\ a_2 \end{pmatrix} = \frac{4\pi\xi}{f_1 + f_2} \begin{pmatrix} f_1 f_2 \\ 1/4\pi^2 \end{pmatrix} \tag{29}$$

where a_1 and a_2 are coefficients of Rayleigh damping; f_1 and f_2 are the first-order and second-order natural frequencies of the structure, respectively. ξ is the damping ratio with a value of 0.02 in this paper.

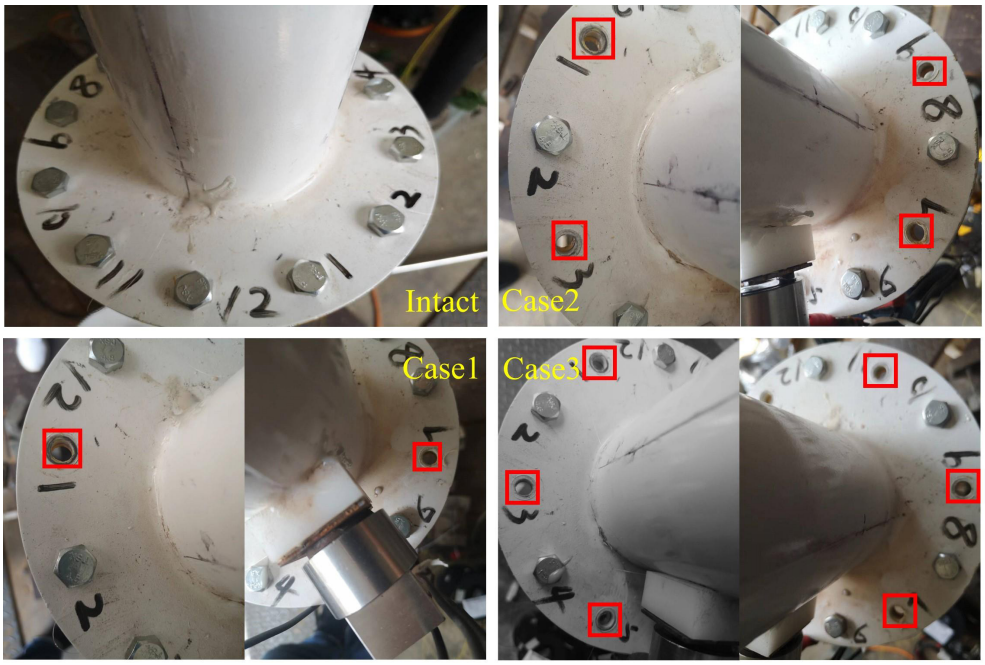

Fig. 21: Number of bolts under different working conditions

Table 4: The natural frequencies of monopile wind turbine model under different working conditions

Case	Number of bolts	Bolt No.	Natural frequencies (Hz)	
			1st	2nd
Intact	N/A	N/A	8.349	41.280
1	2	1,7	7.995	39.664
2	4	1,3,7,9	7.824	36.987
3	6	1,3,5,7,9,11	5.866	29.421

5.4. Model updating results under different working conditions

It should be noted that added masses of accelerometers and the eccentric rotation device significantly impact the dynamic characteristics of the monopile wind turbine. To obtain accurate FE model in different cases, the initial FE model of the intact structure needs to be updated before the stiffness degradation of the flange. The complex exponential decomposition method is applied to decompose and reconstruct the measured vibration response signal.

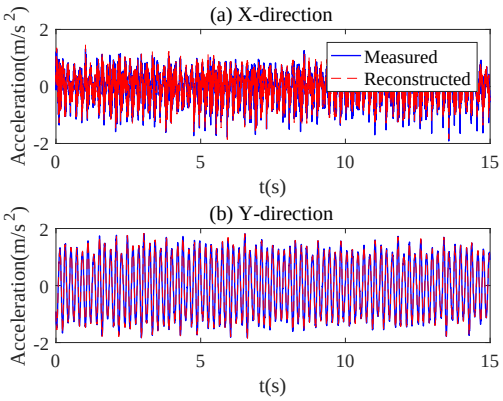

Fig. 22: Reconstructed accelerations of Sensor 1

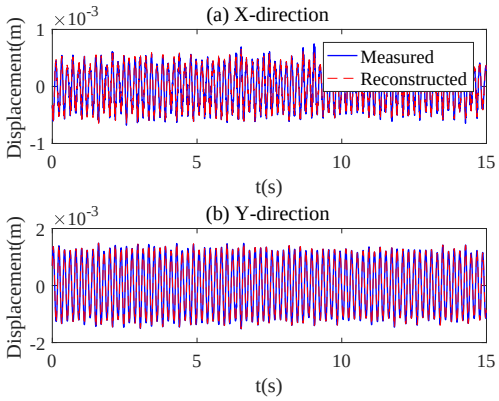

Fig. 23: Reconstructed displacements of (a) Sensor 8; (b) Sensor 9

Taking the Sensor 1, 8 and 9 as an example, it can be observed that the reconstructed signals are in good agreement with the measured data shown in Figs. 22 and 23. The maximum errors between the reconstructed and measured value are 4.333×10^{-2}, 1.454×10^{-2}, 3.518×10^{-5} and 2.241×10^{-5}, respectively, demonstrating the correctness of complex exponential decomposition method for decomposing and reconstructing signal. Taking the translational degree of freedom along the X-direction of the intact structure as an example, results of the first two acceleration components at different times shown in Fig. 24, indicating the variation of structural characteristics.

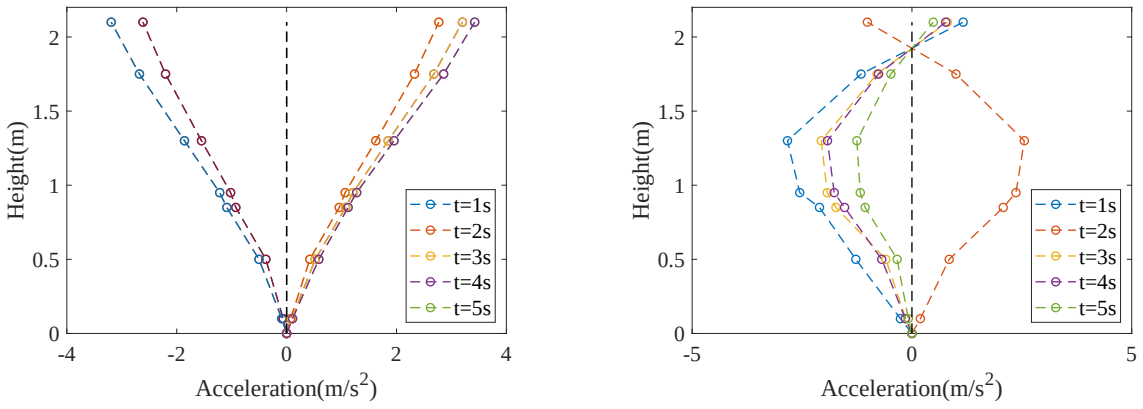

(a) 1-st acceleration components

(b) 2-nd acceleration components

Fig. 24: The acceleration components of intact monopile wind turbine model at different moments

Since the first two modal parameter of the wind turbine structure can be accurately obtained during the test, to weaken the influence of selection of frequency range on the calculation of the updating coefficients. The spectrum curve measured at Sensor 1 in the different ranges of frequencies are shown in Fig. 25. Based on the first two acceleration components of the measured model, the SACs of FRFs are calculated using Eq. (12). In Fig. 26, the SACs in the second frequency Range 2 are small as compared with the results in other ranges, indicating that the FRFs in this frequency band are more sensitive to the structural vibration characteristics. Therefore, the FRFs in the second frequency range are selected for the next calculation of updating coefficients.

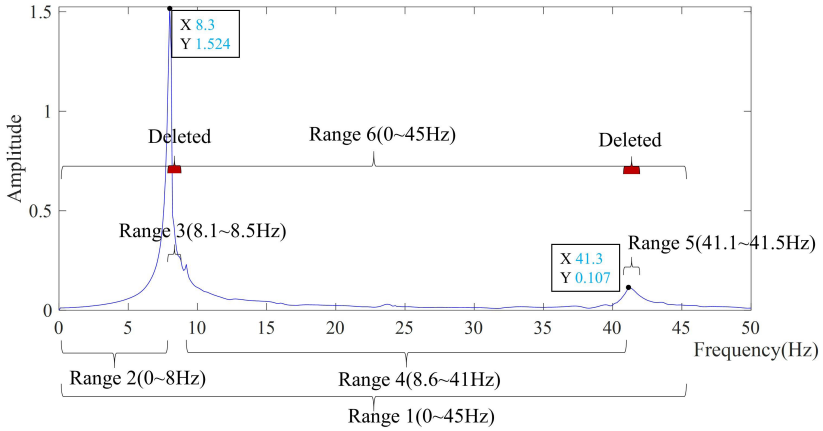

Fig. 25: Division of frequency range for wind turbine model

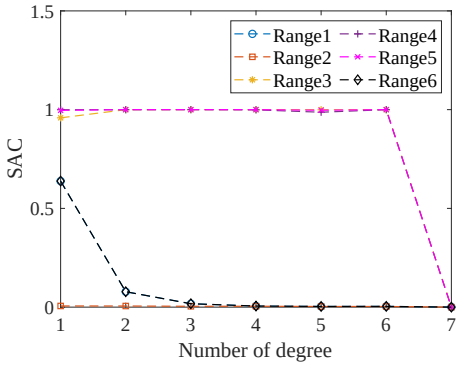

Fig. 26: Division of frequency range for wind turbine model

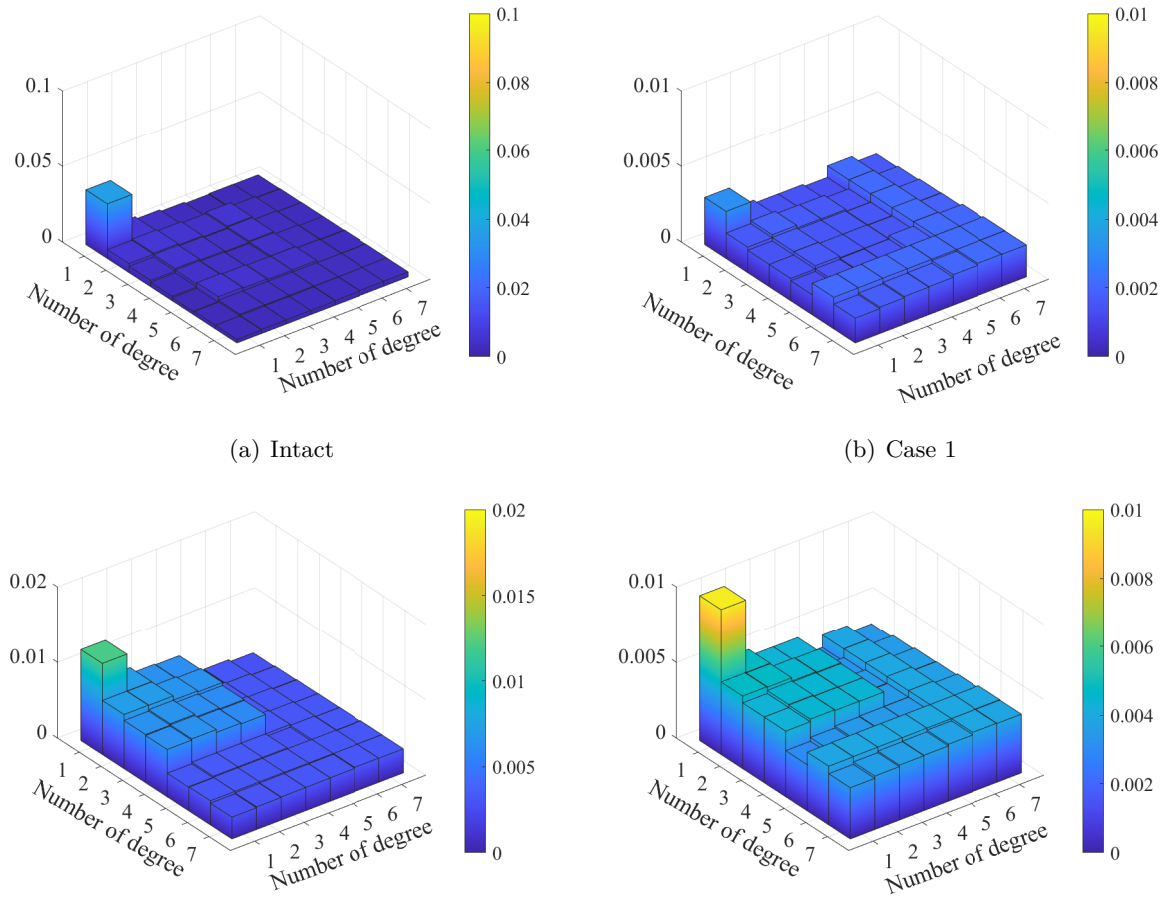

(a) Intact (b) Case 1

(c) Case 2 (d) Case 3

Fig. 27: The SAC of monopile wind turbine model under different cases

Results of the SAC matrix of the complete FRF under different cases are shown in Fig. 27. It can be observed that the maximum SACs in four models are 0.0360, 0.0031, 0.0120 and 0.0096, respectively. As compared with results shown in Fig. 26, the maximum SACs of complete FRF for Range 2 are smaller than the results from other ranges. Employing Eq. (15), the objective function is constructed in a function of SAC and the first two natural frequencies. The updating coefficients of the monopile wind turbine model are calculated using Eqs. (18)∼(25) with the population of 2000 and number of iterations of 100 for the IPSO algorithm, respectively. As shown in Fig. 28, the degree of the stiffness degradation increases as the removed number of bolts at the flange is increased. To evaluate the matching degree between the updated model and the measured structure, the eigenvalue-analysis method is applied to calculate the natural frequencies of the

updated model. It can be observed in Table 5 that the maximum error of the first two natural frequencies is 1.887% in four cases, indicating that the proposed method can accurately calculate the updating coefficients of the monopile wind turbine, and demonstrate the applicability of the proposed method for marine engineering structures.

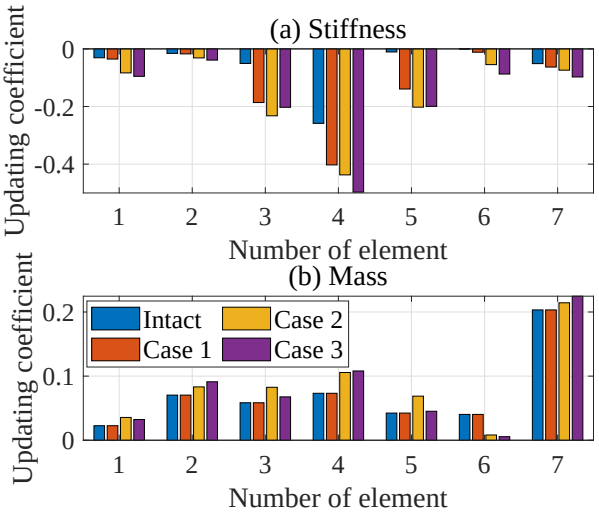

Fig. 28: Number of bolts under different working conditions

Table 5: Natural frequencies of monopile wind turbine model under different working conditions

Case	Mode	Measured(Hz)	Baseline model(Hz)	Relative error(%)	Proposed method(Hz)	Relative error(%)
Intact	1st	8.349	9.222	10.456	8.430	0.970
	2nd	41.280	42.334	2.553	40.501	1.887
1	1st	7.995	9.222	15.347	8.115	1.501
	2nd	39.664	42.334	6.732	39.598	-0.166
2	1st	7.824	9.222	17.868	7.901	0.984
	2nd	37.987	42.334	11.443	38.606	1.630
3	1st	6.269	9.222	47.105	6.383	1.786
	2nd	29.421	42.334	43.890	28.989	1.778

6. Experiment of an offshore jacket platform

To verify the performance of the proposed method for complex offshore structures, an experimental study of a jacket platform is carried out in the Vibration Laboratory at the Ocean University of China. The model is fixed on the ground in the experiment and the shock excitation by a force hammer is applied on the top of the structure.

6.1. Experiment setup

The model is a four-legged, five-layered jacket platform with height of 2200 mm shown in Fig. 29. The parameters of structural elements are listed in Table 6. The twenty accelerometers, which are labelled as Sensor1∼ Sensor20 (OTES-3A-0002) from the top to bottom of the jacket platform, are placed on the top surface of each floor to measure the acceleration response. The acceleration signals are recorded by the CRONOS PL-DCB8 with a sampling frequency of 200 Hz.

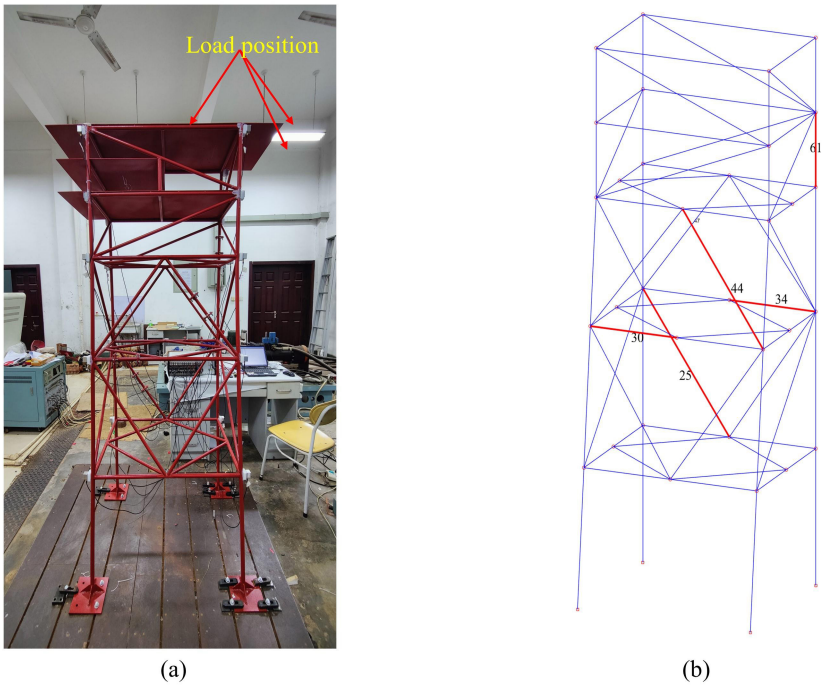

Fig. 29: The diagram of the jacket platform for (a) the experiment; (b) the FE model

Table 6: Dimension of components of of jacket platform

Element type	Sectional dimension
Vertical braces	22 mm×2.2 mm
Lateral braces	19 mm×1.2 mm
Diagonal braces	16 mm×1.2 mm
First deck	1200 mm×500 mm×3 mm
Second deck	600 mm×500 mm×3 mm
Third deck	1000 mm×500mm×3 mm

6.2. Description of the baseline model

The FE model of the jacket platform is constructed using MATLAB. Each lever is meshed by two-node three-dimensional beam elements. Thus, the model has totally 36 nodes and 83 lever elements. To facilitate the analysis, the steel plates modelled as lumped masses are applied on the nodes. The diagram of FE model for the jacket platform is shown in Fig. 29 (b). It is assumed that only the mass and stiffness matrices of the system need to be updated. Using the eigenvalue-analysis method, the first three mode shapes of the FE model are shown in Fig. 30, and the corresponding first three natural frequencies are 9.231 Hz, 12.350 Hz and 18.892 Hz, respectively.

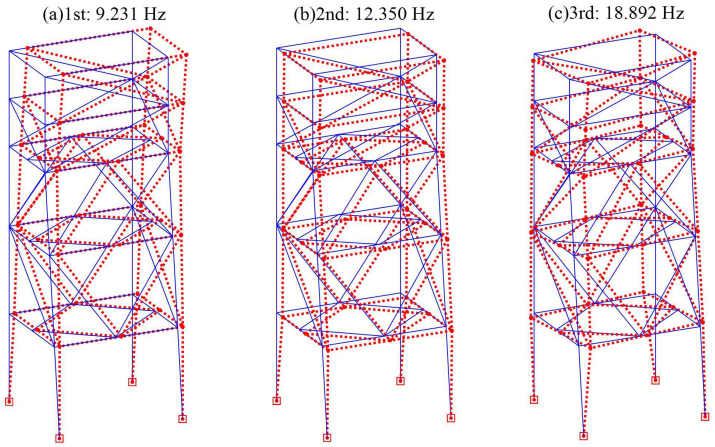

Fig. 30: The mode shape of jacket platform model: (a) 1st (b) 2nd (c) 3rd

6.3. Loads and the working condition

To simulate the variation of structural stiffness in the experiment, the different cross-sectional areas of the replacement are considered in four cases shown in Table 7. An impulse excitation by a hammer is applied to excite the free vibration signal. It is noted that the first three natural frequencies of the model decrease as the number of replacements is increased.

Table 7: The natural frequencies of jacket platform model under different working conditions

Case	Number of replacements	Replacement No.	Natural frequencies (Hz)		
			1st	2nd	3rd
Intact	N/A	N/A	8.643	11.778	15.969
A	1	61	8.467	11.531	15.815
B	3	30,34,61	8.217	11.453	15.759
C	5	25,30,34,44,61	7.951	11.215	15.576

6.4. Discussions

To obtain the accurate FE results of the intact structure as a benchmark solution, the complex exponential method is applied to decompose and reconstruct the acceleration response shown in Fig. 31. The maximum errors between reconstructed and measured acceleration are 2.012×10^{-2}, 3.703×10^{-2}, 6.199×10^{-3}, 1.914×10^{-2}, 4.661×10^{-2}, 8.653×10^{-2}, 6.122×10^{-2} and 6.497×10^{-3}, respectively. It can be concluded that reconstruction results of acceleration responses are in good agreement with measurement values.

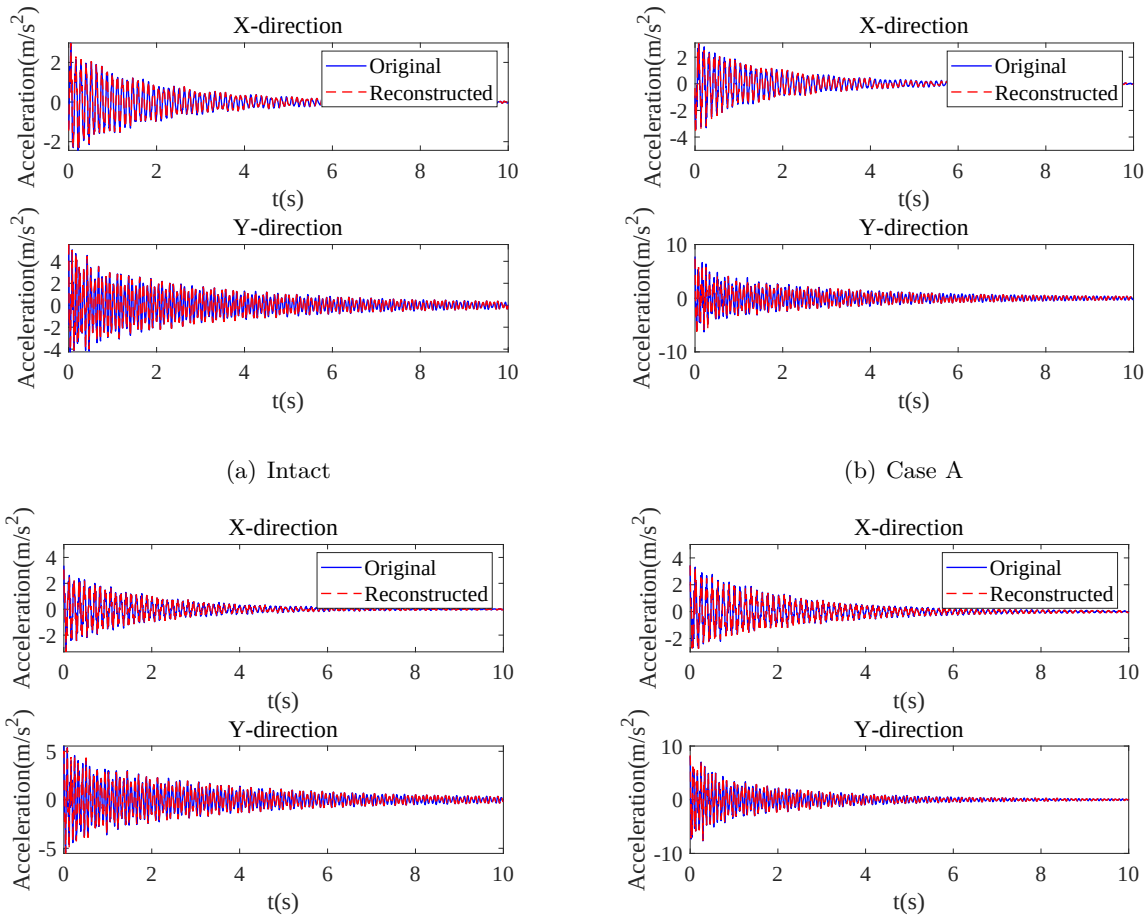

(a) Intact

(b) Case A

(c) Case B

(d) Case C

Fig. 31: Acceleration response signals under different cases

The complete FRFs of the jacket platform can be calculated by Eq. (10), and the results of H_{11}, H_{12}, H_{13} and H_{14} are shown in Fig. 32. It should be noted that the FRFs in different cases greatly differ from the baseline model. To mitigate the influence of the improper selection of FRFs on the accuracy of the updating coefficients, the frequency range is determined by the SAC values. In Fig. 33, the detailed results in the different frequency ranges in Case Intact are provided.

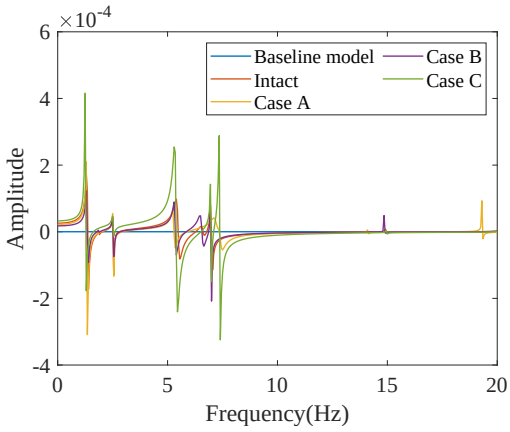

(a) Intact

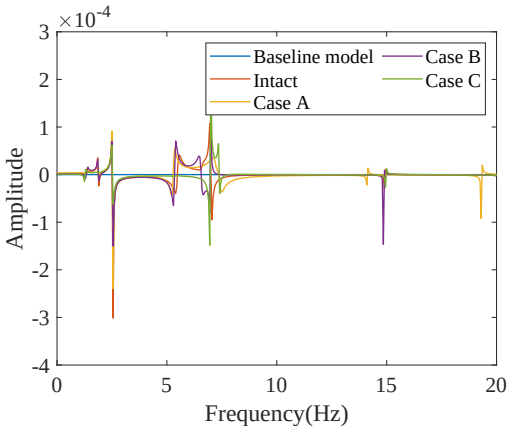

(b) Case A

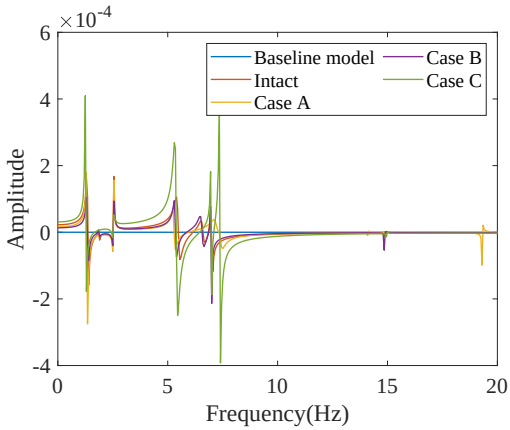

(c) Case B

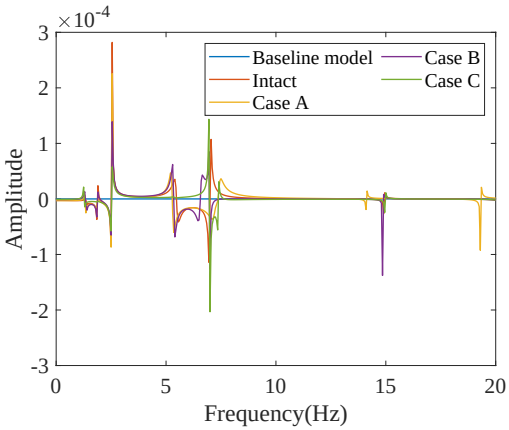

(d) Case C

Fig. 32: Acceleration response signals under different cases

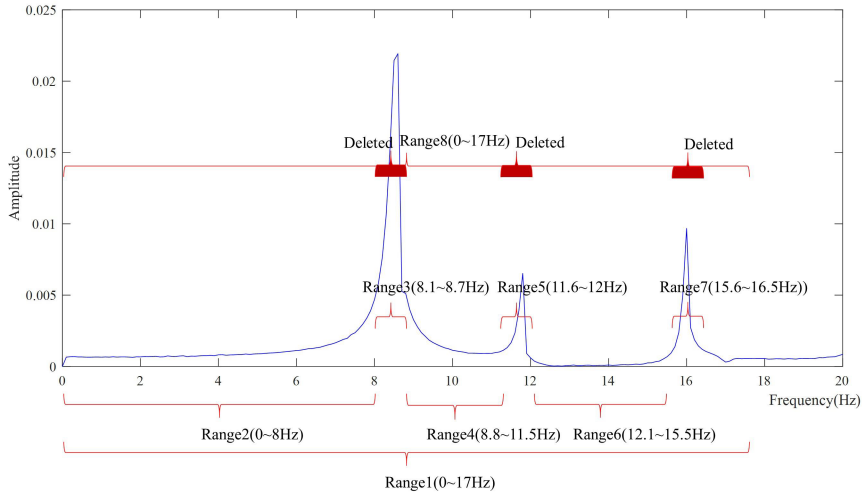

Fig. 33: Division of frequency range for physical jacket platform model

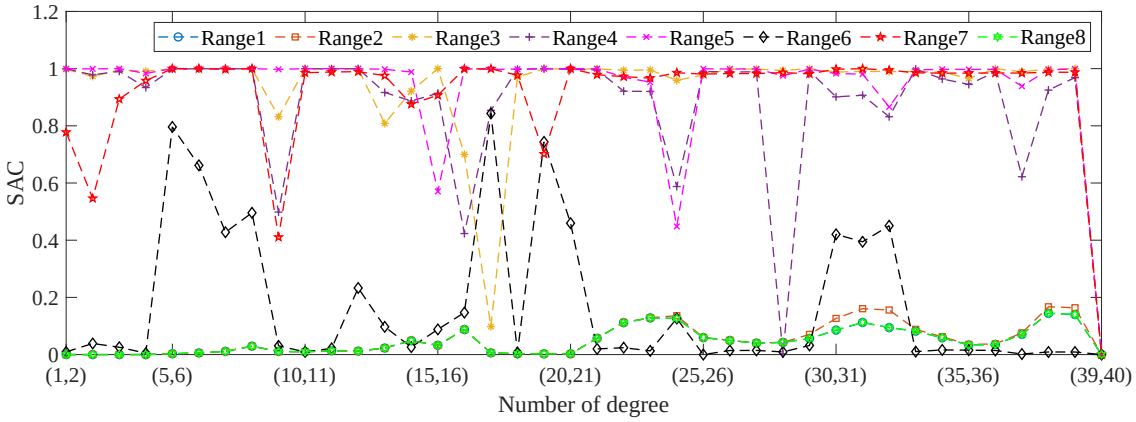

Fig. 34: Division of frequency range for physical jacket platform model

The SACs of adjacent degree of the physical jacket platform are shown in Fig. 34. One can see from Fig. 34 that the results for frequency range 8 are smaller, indicating that FRFs of the FE model in this frequency range are less correlated with the actual structure. Therefore, the FRFs of frequency range 8 are selected in this test to calculate the SACs of complete FRFS, and the results are shown in Fig. 35. It can be observed that the maximum SACs in four cases are 0.587, 0.629, 0.553 and 0.010, indicating that the difference of FRFs between the measured and baseline models are large.

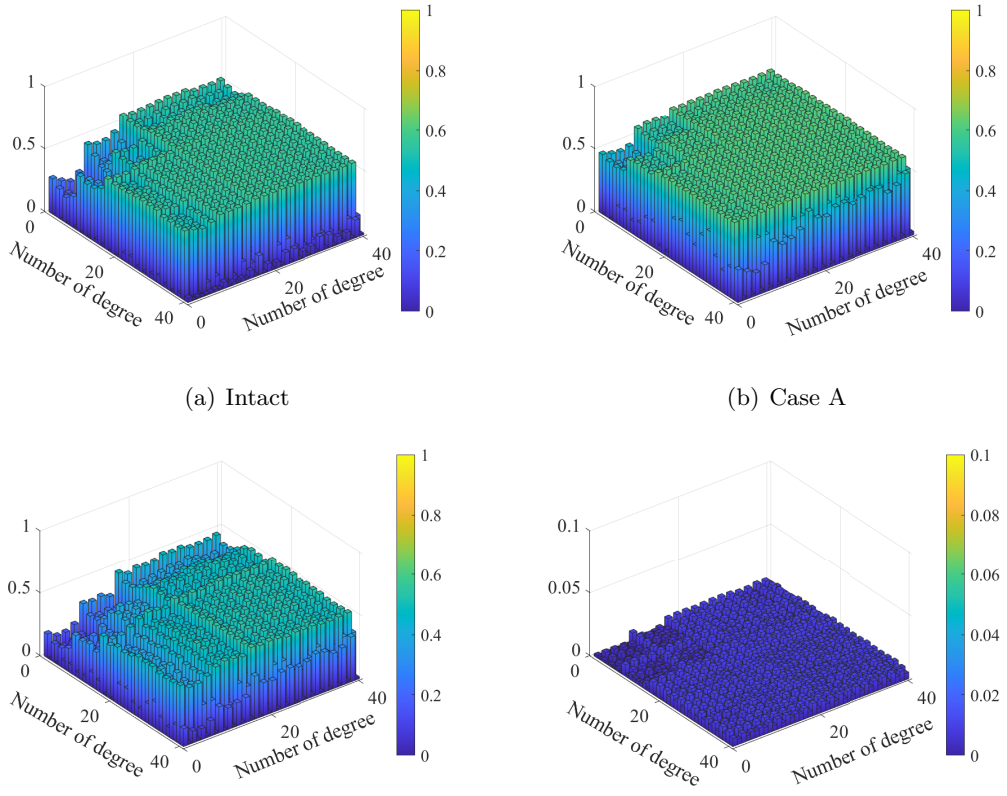

(a) Intact (b) Case A

(c) Case B (d) Case C

Fig. 35: The SAC of jacket platform model before model updating under different cases

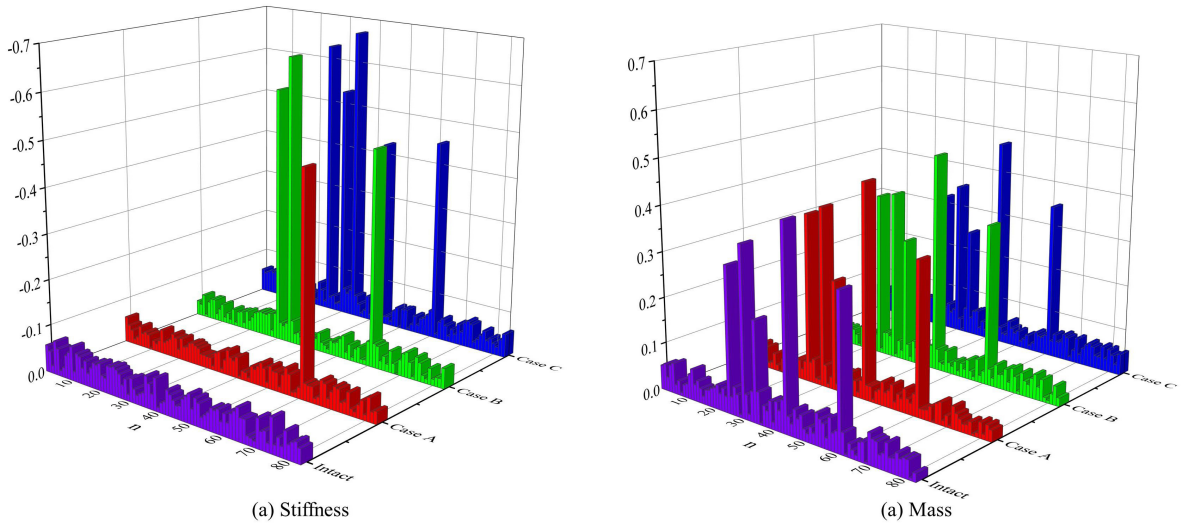

(a) Stiffness (a) Mass

Fig. 36: The updating coefficients of jacket platform model: (a) stiffness (b) mass

Table 8: Natural frequencies and MACs of jacket platform model under different working conditions

Case	Mode	Measured(Hz)	Baseline model(Hz)	Relative error(%)	Proposed method(Hz)	Relative error(%)
Intact	1st	8.643	9.231	6.803	8.780	1.585
	2nd	10.998	12.350	4.857	10.704	2.673
	3rd	15.969	18.892	18.304	16.591	3.895
A	1st	8.467	9.231	9.023	8.590	1.453
	2nd	10.731	12.350	7.103	10.467	-2.460
	3rd	15.815	18.892	19.456	16.187	2.352
B	1st	8.217	9.231	12.340	8.188	-0.353
	2nd	10.453	12.350	7.832	9.948	4.831
	3rd	15.759	18.892	19.881	15.149	3.871
C	1st	7.951	9.231	16.099	7.864	-1.094
	2nd	10.115	12.350	10.120	9.703	-4.073
	3rd	15.576	18.892	21.289	16.064	3.133

The optimal updating coefficients of the jacket platform are achieved using the IPSO algorithm with the population of 5000 and generation of 100. The updating coefficients of the model in four cases are shown in Fig. 36. To evaluate the consistency between the updated model and the physical structure, the eigenvalue-analysis is carried out to calculate the natural frequencies of the updated model. It can be observed in Table 8 that the maximum errors of the first three natural frequencies in four cases are 3.895%, -2.460%, 4.831% and -4.073%, demonstrating the effectiveness and accuracy of the proposed method applicable for complex marine structures.

7. Conclusions

In the paper, a model updating method based on the normalized acceleration components has been proposed using the extended frequency response functions and global optimization technique.The effectiveness and robustness of the method has been demonstrated throughout three examples. In the numerical example of a jacket platform, the remarkable consistency between the updated and theoretical models has been achieved under the effect of 5% noise. To solve a practical

problem in the area of marine engineering, the proposed method can accurately calculate the updating coefficients of the monopile wind turbine with the maximum error of the natural frequency is 1.887% under different cases. In the experimental tests of the offshore jacket platform, results have indicated that the proposed method has a good capacity to accurately update the model under the influence of the spatial incompleteness.

However, the slightly low computational efficiency and large amount of computer resources of the proposed method have been observed. Also, the developed method can only resolve problems associated with the model updating of linear structures. Furthermore, future work including the model updating considering the effects of the environmental conditions, measurement noise, nonlinear and spatial incompleteness will be carried out to enhance the existing method applicable to various marine engineering structures. In summary, the proposed method has provided a useful insight into the development of effective and robust techniques for model updating of complex structures in marine engineering.

8. CRediT authorship contribution statement

FushunLiu: Conceptualization, Methodology, Writing-review & editing. **XingguoLi**: Investigation, Validation, Writing-original draft. **HongSong**: Writing-review, editing. **DianziLiu**: Analysis, Discussion, Writing-review,& editing.

9. Declaration of Competing Interest

We declare that we have no financial and personal relationships with other people or organizations that can inappropriately influence our work, there is no professional or other personal interest of any nature or kind in any product, service and/or company that could be construed as influencing the position presented in, or the review of, the manuscript.

10. Acknowledgements

The authors acknowledge the financial support by the National Natural Science Foundation-Basic Science Center Project (52088102), the National Outstanding Youth Science Fund Project of National Natural Science Foundation of China (52125106).

11. References

Arora, V., 2014. Structural damping identification method using normal FRFs. International Journal of Solids and Structures, 51(1), 133–143.

Arora, V., Singh, S. P., Kundra, T. K., 2009a. Finite element model updating with damping identification. Journal of Sound and Vibration, 324(3-5), 1111–1123.

Arora, V., Singh, S. P., Kundra, T. K., 2009b. On the use of damped updated FE model for dynamic design. Mechanical Systems and Signal Processing, 23(3), 580–587.

Bartilson, D. T., Jang, J., Smyth, A. W., 2020. Symmetry properties of natural frequency and mode shape sensitivities in symmetric structures. Mechanical Systems and Signal Processing, 143, 106797.

Begambre, O., Laier, J. E., 2009. A hybrid Particle Swarm Optimization – Simplex algorithm (PSOS) for structural damage identification. Advances in Engineering Software, 40(9), 883–891.

Canbaloğlu, G., Özgüven, H.N., 2016. Model updating of nonlinear structures from measured FRFs. Mechanical Systems and Signal Processing, 80, 282-301.

Craig, R., Kurdila, A., 2006. Fundamentals of Structural Dynamics, second Ed. John Wiley & Sons Inc., NewYork, USA.

Esfandiari, A., Bakhtiari-Nejad, F., Rahai, A., Sanayei, M., 2009. Structural model updating using frequency response function and quasi-linear sensitivity equation. Journal of Sound and Vibration, 326(3-5), 557–573.

Friswell, M., Mottershead, J.E., 1995. Finite Element Model Updating in Structural Dynamics,Vol. 38. Springer Science & Business Media.

Guo, H. Y., Li, Z. L., 2009. A two-stage method to identify structural damage sites and extents by using evidence theory and micro-search genetic algorithm. Mechanical Systems and Signal Processing, 23(3), 769–782.

Hasselmann K., et al., 1973. "Measurements of wind-wave growth and swell decay during the Joint North Sea Wave Project (JONSWAP)". Deutschen Hydrographischen Zeitschrift Reihe, 8, 12

Hong, H., Pu, Q. H., Wang, Y., Chen, L. J., Gou, H. Y., Li, X. B., 2017. Model-updating with experimental frequency response function considering general damping. Advances in Structural Engineering, 136943321770678.

Jiang, D., Zhang, P., Fei, Q., Wu, S., 2014. Comparative study of model updating methods using frequency response function data. Journal of Vibroengineering, 16(5):2305-2318.

Li, H., Liu, F., Hu, S.-L. J., 2008. Employing incomplete complex modes for model updating and damage detection of damped structures. Science in China Series E: Technological Sciences, 51(12), 2254–2268.

Li, X., Liu, F., 2022. A nonmode-shape-based model updating method for offshore structures using extracted components from measured accelerations. Applied Ocean Research, 121, 103087.

Lin, R. M., Zhu, J., 2006. Model updating of damped structures using FRF data. Mechanical Systems and Signal Processing, 20(8), 2200–2218.

Liu, F., 2011. Direct mode-shape expansion of a spatially incomplete measured mode by a hybrid-vector modification. Journal of Sound and Vibration, 330(18-19), 4633–4645.

Liu, F., Li, H., 2013. A two-step mode shape expansion method for offshore jacket structures with physical meaningful modelling errors. Ocean Engineering, 63, 26-34.

Liu, F., Li, H., Li, W., Wang, B., 2014. Experimental study of improved modal strain energy method for damage localisation in jacket-type offshore wind turbines. Renewable Energy, 72, 174-181.

Liu, F., Yang, Q., Li, H., Li, W., Wang, B., 2016. Discrepancy study of modal parameters of a scale jacket-type supporting structure of 3.0-MW offshore wind turbine in water and in air. Renewable Energy, 89, 60-70.

Lu, Y., Tu, Z., 2004. A two-level neural network approach for dynamic FE model updating including damping. Journal of Sound and Vibration, 275(3-5), 931-952.

Majumdar, A., Maiti, D. K., Maity, D., 2012. Damage assessment of truss structures from changes in natural frequencies using ant colony optimization. Applied Mathematics and Computation, 218(19), 9759-9772.

Modak, S. V., Kundra, T. K., Nakra, B. C., 2002. Comparative study of model updating methods using simulated experimental data. Computers & Structures, 80(5-6), 437-447.

Mottershead, J. E., Friswell, M. I., 1993. Model Updating In Structural Dynamics: A Survey. Journal of Sound and Vibration, 167(2), 347-375.

Ngan, J. W., Caprani, C. C., Bai, Y., 2019. Full-field finite element model updating using Zernike moment descriptors for structures exhibiting localized mode shapes. Mechanical Systems

and Signal Processing, 121, 373-388.

Pradhan, S., Modak, S. V., 2012. Normal response function method for mass and stiffness matrix updating using complex FRFs. Mechanical Systems and Signal Processing, 32, 232-250.

Sanayei, M., Imbaro, G. R., McClain, J. A. S., Brown, L. C., 1997. Structural Model Updating Using Experimental Static Measurements. Journal of Structural Engineering, 123(6), 792-798.

Tu, Z., Lu, Y. 2008., FE model updating using artificial boundary conditions with genetic algorithms. Computers & Structures, 86(7-8), 714–727.

Zhang, Q., Hou, J., An, X., Jankowski, Ł., Duan, Z., Hu, X., 2023. Vehicle parameter identification based on vehicle frequency response function. Journal of Sound and Vibration. 542, 117375.

Zhang, Y., Guo, J., Zhou, Q., Wang, S., 2021. Research on damage identification of hull girder based on Probabilistic Neural Network (PNN). Ocean Engineering, 238, 109737.